Translated from *Uspekhi Khimii*, 48, 448-480 (1979) U.D.C. 546.422

Non-stoichiometry of the Alkaline Earth Metal Oxides

P.V.Kovtunenko and Ya.L.Kharif

Experimental data on the departure from stoichiometry in the alkaline earth metal oxides (MO) have been summarised and analysed. The $p-T-x$ diagram of BaO, and the equilibrium diagrams of the intrinsic atom defects in BaO and SrO, have been constructed. The relationship between the properties of the surface of MO crystals and their ability to emit electrons has been examined. The bibliography contains 94 references.

CONTENTS

I.	Introduction	243
II.	Experimental data on the departure from stoichiometry in alkaline earth metal oxides	243
III.	Some thermodynamic properties of MO crystals	248
IV.	Nature of the intrinsic atom defects in MO	254
V.	Properties of the surface and nature of the emitting power of MO crystals	257

I. INTRODUCTION

The alkaline earth metal oxides (MO) are widely used as electron-emitting coatings on thermionic-cathodes, and have been the objects of a large number of physico-chemical studies. The properties of the alkaline earth metal oxides, such as the ability to emit electrons, electrical conductivity, photo-conductivity, luminescence, etc., are extremely sensitive to change in the composition of the MO, that is to departures from stoichiometry. Thus studies of the dependence of the composition of non-stoichiometric MO crystals on the thermodynamic parameters of the state of the "crystal–vapour" system carried out in the past ten years in the Soviet Union and in other countries are of considerable theoretical and practical importance.

The present review summarises available experimental data on the direct determination of the departure from stoichiometry, and compares and analyses the data in order to build up from the isolated fragments, as far as possible, a more complete picture of the state of MO crystals in equilibrium with their vapour. The summary and analysis of the experimental data are also important in relation to the general questions of the chemistry of non-stoichiometric crystals and the problems of investigating the nature of the strong emitting power of MO crystals.

II. EXPERIMENTAL DATA ON THE DEPARTURE FROM STOICHIOMETRY IN ALKALINE EARTH METAL OXIDES

Thermodynamic analysis of the phenomena arising in the distribution of the components of a crystal between the vapour and solid phases shows that a certain quantity of M and O must be present in MO crystals and on their surface in a state different from the usual state of M and O forming the crystal of the compound and occupying regular sites of the crystal lattice. This difference is revealed, in particular, in the difference in the chemical properties of these states of the metal and oxygen in their reactions with water, acids, etc. These components of the MO will subsequently be described as excess if the concentration of one of them is greater than that of the other or quasi-excess if they are equal, irrespective of the location of these components in the crystal. The differences in the chemical and physicochemical properties of the excess components have made it possible to develop methods for their direct quantitative determination[1-8].

1. Excess Metal in MO. Influence of the Surface of the Crystals on the Concentration of Excess Metal in a Non-stoichiometric Specimen

The study of the phenomena leading to the production of an excess of metal in MO began with attempts to determine the factors responsible for the high emitting power of oxide cathodes. A large number of studies in the Soviet Union[1,9-14] and other countries[15-20] showed that the high electron emission of oxide cathodes is in fact due to the production of excess M in the bulk and on the surface of the oxide crystals. The technical difficulties associated with studies of real cathodes, however, made it impossible to obtain reliable quantitative data on the dependence of the equilibrium concentration of the excess metal in MO on the conditions of synthesis of the material, in particular the vapour pressure and temperature. These data were obtained in the study of the physico-chemical properties of the pure oxides away from the cathodes.

The solubility of Ba in the bulk of BaO crystals was first measured in 1937 by Schriel[2], and later by Kane[3] and Libowitz[4], who by chemical analysis measured the excess Ba in BaO crystals grown from a solution of BaO in liquid Ba. According to Schriel, the solubility of Ba in BaO at 1150° is 0.5–1.2 at.%. Libowitz[4] believes that this value is slightly too high, because of experimental errors in the determination of Ba. Kane[3] and Libowitz[4] found that at 890–910° the solubility is 0.07–0.12 at.%.

Studies of importance for understanding the formation of non-stoichiometric MO crystals were carried out using single crystals grown from the vapour phase[3-6,21,22]. In particular, it was shown[5,21,22] that the excess Ba in BaO creates two types of impurity centre, corresponding to two peaks in the absorption spectra, at 2.0 eV (blue crystals) and at 1.2 eV (red crystals). Red BaO crystals were obtained by heating colourless BaO crystals in liquid Ba, and blue crystals by heating in Ba vapour. Timmer[6] found that the concentration of colour centres with an absorption maximum at 2.0 eV, calculated using Smakula's

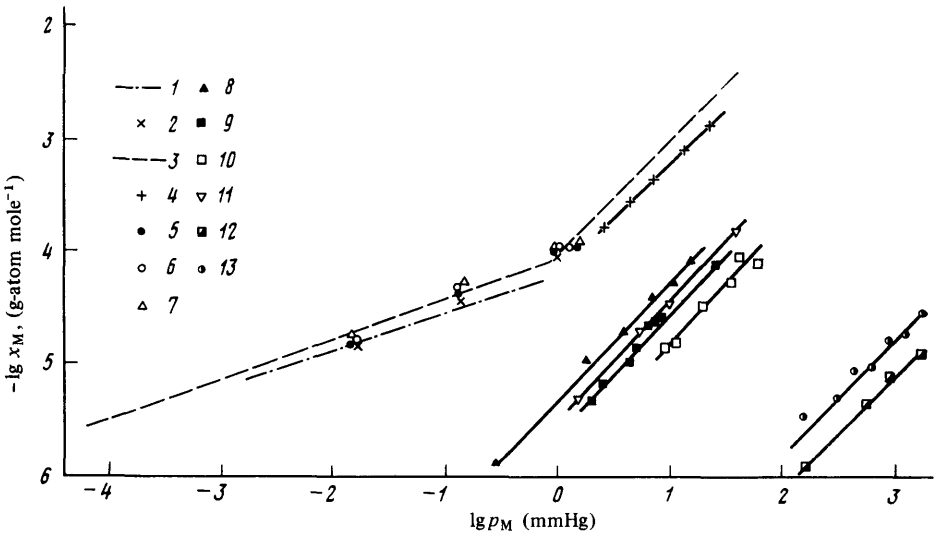


Figure 1. Solubility of excess metal in MO. Solubility isotherms for Ba in BaO at 1150° (*1*—from Ref. 6, *2*—from Ref. 29), at 1200° (*3*—from Ref. 39, *4*—from Ref. 40), at 1250° (*5*—from Ref. 29), at 1350° (*6*—from Ref. 29), and at 1450° (*7*—from Ref. 29). Solubility isotherms for Sr in SrO [28] (*8*— at 1143°, *9*—at 1238°, *10*—at 1320°). Solubility isotherm for Ca in CaO [29] (*11*) at 1700°). Solubility isotherms for Mg in MgO [29] (*12*—at 1612°, *13*—at 1813°).

equation[23], is proportional to the vapour pressure of Ba to the power 1/3. Chemical analysis of the excess Ba in blue BaO crystals[5] showed that its concentration is approximately equal to the concentration of colour centres. Thus Timmer's results were taken to indicate that the solubility of excess Ba in BaO depends on the Ba vapour pressure. The solubility isotherm obtained by Timmer at 1150°, corrected using new data on the vapour pressure of Ba, [24,25] is given in Fig. 1.

Hensley and coworkers[8,26-29] used the same experimental techniques as Timmer to study the non-stoichiometry of MO. The absorption spectra of additively coloured crystals of MgO, CaO, SrO, and BaO showed two impurity absorption bands analogous to those observed by Sproull and coworkers[5]. For the more intense of the two bands, the concentrations of the colour centres were calculated using the equations of Dexter[30] and Smakula[23]. For MgO, [26] CaO, [27] and SrO [28] these were the bands at longer wavelengths, corresponding to photon energies 5.0, 3.1, and 2.5 eV respectively, and for BaO it was the band at shorter wavelength (2.0 eV). The results of the calculations are given in Fig. 1. According to these data, the concentration of colour centres is proportional to p_M to the first power for MgO, CaO, and SrO, and for BaO the exponent lies between 1/2 and 1/3. BaO, [29] SrO, [28] and MgO [26] were studied at several temperatures, to obtain the temperature dependence of the concentration of colour centres. For BaO and MgO, the concentration of colour centres increased slightly with temperature in the range studied, 1150–1450°, and for SrO it decreased.

In the study of the formation of non-stoichiometric crystals, it must be borne in mind that the thermodynamic properties of the crystals are different in the bulk and on the surface of the crystals, that is at the "solid–gas" interface. As a result, the concentration of excess component is different on the surface and in the bulk of the crystals. For single crystals, or large crystals in general, the contribution of the excess component localised on the surface to the total departure from stoichiometry will be negligible. It will be expected to increase, considerably, however, on going to specimens having highly developed surfaces, that is powders. In 1962, the present author[10,31,32] in fact found that in powdered specimens synthesised by heating to equilibrium at 1150° in oxygen at a pressure of 10^{-8} mmHg, not less than 90% of the total excess Ba produced in the crystals was localised on the surface of the crystallites, the average size of which was several microns. The preferential localisation of Ba on the surface of powdered BaO was also established in later work[33]. Approximately the same picture was observed on zinc oxide[34,35].

This phenomenon was studied in detail for BaO and SrO, [36,37] using powdered oxide specimens prepared by the same methods[10,31,32], having a specific surface of 0.6 m^2 g^{-1}. The excess metal was determined by the gas-volumetric method first proposed by Berdennikova[1]. The substance was dissolved in water, and the quantity of hydrogen liberated in the reaction of the excess metal with water was determined. The improved method of measurement gave the analysis a sensitivity of 2×10^{-8} g-atom Ba per mole of BaO. The BaO and SrO specimens were heated for prolonged periods at 1000–1150° and $p_{O_2} = 3\times10^{-8}$–1×10^{-5} mmHg until equilibrium was established. Analysis showed that the product contained excess metal. The isothermal dependence of the concentration of excess metal on p_M (p_M was calculated from the given oxygen pressure and the known dissociation constant of the oxide K_{MO}) is shown in Figs. 2 and 3. The form of the isotherms obtained is typical of adsorption isotherms[38]. It may therefore be assumed that they correspond to processes taking place chiefly on the surface of the crystals and approaching saturation in the region of the inflection on the isotherms. To determine separately the quantities of excess metal located on the surface and

dissolved in the bulk of the crystals, the non-stoichiometric specimens, before the determination of the excess metal, were treated with oxygen at room temperature to remove the excess of metal on the surface without influencing that dissolved in the bulk. As in other experiments[10,31,32], these studies showed that not less than 90% of the excess metal is in fact located on the surface of the crystals, and only about 10% is dissolved in the bulk.

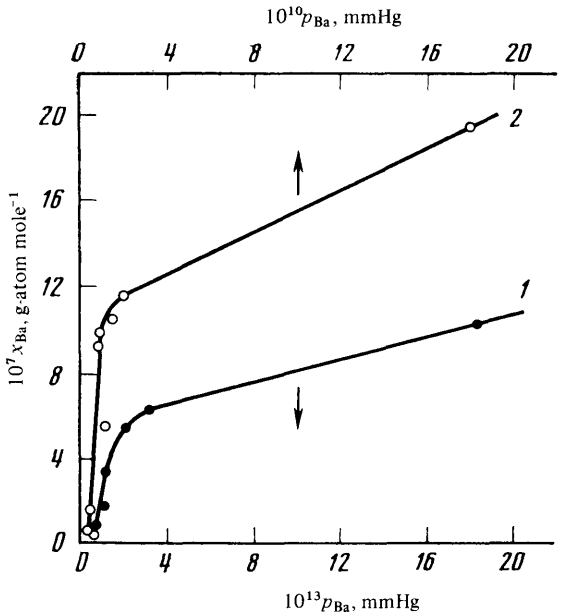


Figure 2. Dependence of the concentration of excess Ba in BaO on the vapour pressure of Ba [36] at 1000° (*1*) and 1150° (*2*).

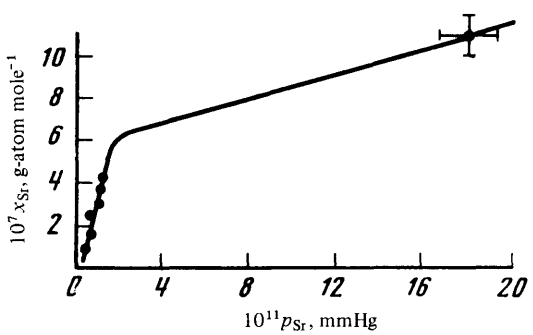


Figure 3. Dependence of the concentration of excess Sr in SrO on the vapour pressure of Sr [37] at 1150°.

At higher M vapour pressures, when the total concentration of excess metal increases chiefly as a result of its dissolution in the bulk, the proportion of excess M due to adsorption on the surface relative to the total concentration of M in the specimen was found to be small. This was confirmed experimentally[39] in a study of the distribution of Ba between the vapour phase and powdered BaO at 1200° in the Ba vapour pressure range 3×10^{-5}–35 mmHg. BaO was saturated with barium using a stream of metal vapour, carried over BaO using helium. The results of the measurements are given in Fig. 1. The experimental points on coordinates $\lg x_{Ba}-\lg p_{Ba}$ are described by two straight lines intersecting at a pressure of ~1 mmHg. In the vapour pressure range 3×10^{-5}–1 mmHg, the equation for the isothermal relationship obtained has the form:

$$x_{Ba} = 7{,}51\cdot10^{-5}p_{Ba}^{0{,}328}, \quad (1)$$

and in the pressure range 1–32 mmHg:

$$x_{Ba} = 1{,}17\cdot10^{-4}p_{Ba}^{1{,}075} \quad (2)$$

(here and subsequently, the solubility is given in g-atom Ba per mole of BaO, and the pressure in mmHg).

In the vapour pressure range 10^{-5}–1 mmHg, the data obtained for powdered specimens[39] show good agreement with the results obtained using single crystals[6,29], indicating that in the pressure range studied, most of the excess Ba is in the bulk of the BaO crystals, and the quantity on the surface is comparatively small. Extrapolation of the data[39] on the solubility of barium in BaO to lower pressures, 10^{-10}–10^{-8} mmHg, shows satisfactory agreement with the data previously obtained for this range[36,37]. In fact, calculation of the concentration of excess barium using Eqn. (1) gives for a pressure of 10^{-9} mmHg the value 0.9×10^{-7} g-atom Ba per mole of BaO, which is about 6% of the total obtained under these conditions in earlier work[36,37] (Fig. 2), and which corresponds approximately to the concentration of excess barium in BaO crystals, remaining in the dissolved state after the surface is cleaned using oxygen. The data[39] for the pressure range above 1 mmHg are close to those obtained earlier[40], but are apparently more accurate, since they were obtained by an improved procedure. The dependence of the solubility on p_{Ba} in this range is the same as for Sr in SrO, [28] Ca in CaO, [27] and Mg in MgO [26] at high metal vapour pressures (see Fig. 1).

2. Excess Oxygen in MO

The most extensive early study of the reaction of BaO with O_2 is that of Hildebrand[41]. In a study of the equilibrium in the BaO–O_2 system in the range 700–800° at oxygen pressures of 10–800 mmHg, Hildebrand found that the solubility isotherms for oxygen in BaO showed two bivariant regions with a univariant region between them, corresponding to equilibrium between two conjugate solid solutions, based on BaO and on BaO_2.

Detailed studies of the solubility of oxygen in BaO and SrO have been carried out in the past ten years in the Mendeleev Moscow Institute of Chemical Technology[42–45]. The equilibria have been studied over a wide range of temperatures and oxygen pressures by a static method in which the quantity of oxygen absorbed by the substance was determined from the decrease in pressure in a known volume.

The solubility of O_2 in BaO was studied at 683–798° and high oxygen pressures (10–500 mmHg).[42] Like Hildebrand[41], the authors cited[42] observed a change in the number of thermodynamic degrees of freedom of the BaO–O_2 system with increase in p_{O_2} under isothermal

conditions (Fig. 4). It was assumed[42] that in the bivariant equilibrium ranges there is one phase in the solid state, interpreted as either a solution of BaO_2 in BaO (first bivariant range) or a solution of BaO in BaO_2 (second bivariant range). For the investigation of the conditions of formation of non-stoichiometric BaO crystals containing excess oxygen, the first bivariant region (I in Fig. 4) is of greatest interest. Under these conditions, the solubility isotherms were described by equations of the form

$$x_O = K_O p_{O_2}^{1/n}; \quad n = 0.88 \div 1.03. \tag{3}$$

The solubility of oxygen in BaO varied in the range 4×10^{-3}–6×10^{-2} mmHg, depending on the conditions of the experiment. Treatment of the data[42] on the solubility of oxygen in BaO in region I (Fig. 4) made it possible to describe them by the analytical equation

$$x_O = 6.6 \cdot 10^{-8} p_{O_2}^{1.0} \exp(+1.61 \cdot 10^4/RT). \tag{4}$$

The temperature coefficient of Eqn. (4) shows that an exothermic chemical reaction takes place when oxygen dissolves in BaO under the above conditions. Thus with increase in temperature the concentration of dissolved oxygen decreases.

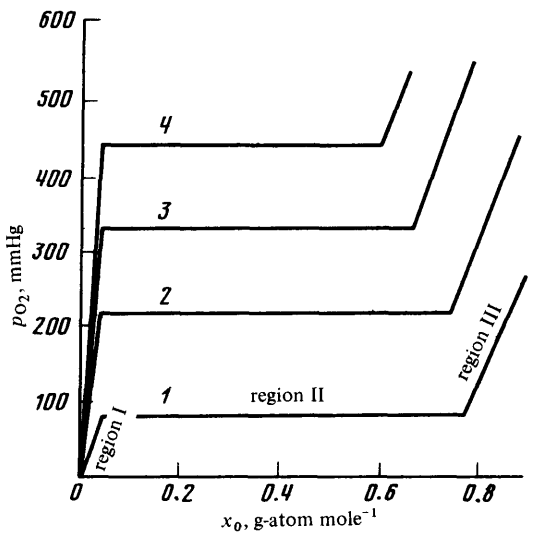


Figure 4. Solubility isotherms for oxygen in BaO [42] at 683° (*1*), 748° (*2*), 773° (*3*), and 790° (*4*).

In the range of the univariant equilibrium (region II in Fig. 4), the temperature dependence of the equilibrium pressure of oxygen above the product of the reaction of BaO with O_2 is given by the equation

$$\lg p_{O_2} = -7500/T + 9.705. \tag{5}$$

The heat of the chemical reaction by which BaO_2 is formed,

$$BaO + 1/2\,O_2 = BaO_2, \tag{6}$$

calculated from the compositions of the conjugate solid solutions and the oxygen pressure in the univariant range, was 18.8 kcal mole^{-1}, in agreement with the value 19.1 kcal mole^{-1}, obtained later[46].

A procedure basically similar to that described above was used to obtain the isothermal dependence of the solubility of O_2 in BaO at 950° and 1150° in the range $p_{O_2} = 2\times10^{-5}$–5 mmHg (Fig. 5).[43] For the oxygen pressure range 5×10^{-4}–5 mmHg, in which the accuracy of the measurements was ±10%, the solubility isotherms were given by the following equations

$$x_O = 1.88 \cdot 10^{-3} p_{O_2}^{1/1.97} \text{ (at 950°)} \tag{7}$$

$$x_O = 9.8 \cdot 10^{-4} p_{O_2}^{1/2.09} \text{ (at 1150°)}. \tag{8}$$

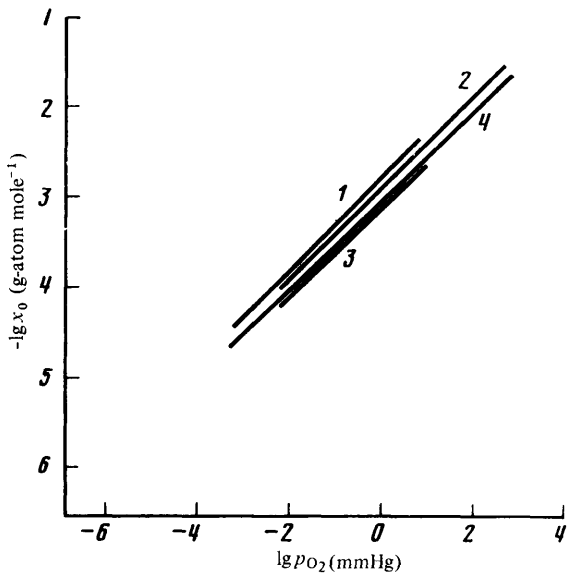


Figure 5. Solubility isotherms for oxygen in BaO at 950° (*1*—from Ref. 43, *2*—from Ref. 47) and at 1150° (*3*—from Ref. 43, *4*—from Ref. 47).

In a later analogous study[47], the solubility of oxygen in BaO was measured at 850–1420° and $p_{O_2} = 5\times10^{-3}$–600 mmHg. The concentration of O_2 absorbed by the oxide was determined by thermogravimetric analysis (TGA) and from the quantity of oxygen liberated when the specimen was dissolved completely in water. The results obtained by these two methods did not coincide, the solubility values obtained from the thermogravimetric measurements being 2–2.5 times those obtained from the gas-volumetric measurements. The former appear more reliable, since in the determination of O_2 by the second method, loss of oxygen as a result of the simultaneous freezing of O_2 and water in the trap cooled by liquid nitrogen is possible. The results obtained by TGA are given in Fig. 6, and are described analytically by the equation

$$x_O = 2.71 \cdot 10^{-5} p_{O_2}^{1/2} \exp(+9080/RT). \tag{9}$$

To measure the bulk absorption of O_2 and its adsorption separately, finely dispersed and coarsely crystalline BaO powders were used[47]. The results of the measurements in the two cases did not differ greatly, indicating that

adsorption makes a relatively small contribution to the measured value of the absorption under the conditions of the experiment.

Comparison shows that these results[43,47] are in agreement (Fig. 5). It should be noted, however, that at $x_O > 2\times10^{-2}$ g-atom O per mole of BaO, the isotherms obtained in one case[47] become steeper (Fig. 6). This apparently indicates that with increase in the concentration of oxygen dissolved in BaO, the law governing the distribution of oxygen between the gaseous phase and the BaO crystals changes.

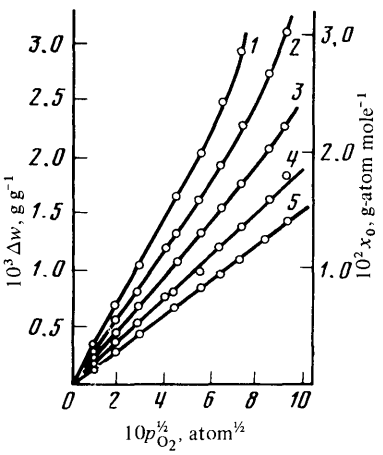


Figure 6. Dependence of the change in weight (Δw) of BaO specimens on the oxygen pressure at 857° (*1*), 927° (*2*), 1027° (*3*), 1127° (*4*), and 1227° (*5*).[47]

Table 1. Coefficients K_O and n in Eqn. (3).[45]

T, °C	700	800	950	1150
10^4K_O	2.77	1.71	1.23	0.93
n	2.37	2.61	2.63	2.66

The SrO–O_2 system was studied in detail at temperatures up to 600° in the range of oxygen pressures 1–100 atm.[48] A range of existence of bivariant equilibria similar to those found in the BaO–O_2 system could not be detected[48]; the stability of SrO_2 was found to be much lower than that of BaO_2.

The solubility of O_2 in SrO was studied[44,45] at 700–1150° and $p_{O_2} = 1\times10^{-5}$–5 mmHg by the method used for BaO.[42,43] The experimental points on coordinates $\lg x_O - \lg p_{O_2}$ were given by straight lines, within the limits of their scatter. The coefficients K_O and n in Eqn. (3), describing the experimental data, are given in Table 1.

Comparison of the solubility of oxygen in SrO and BaO shows that it is lower by approximately an order of magnitude in SrO. As in the case of BaO, however, the solubility of oxygen decreases with increase in temperature.

The data on the solubility of oxygen in MgO [49,50] and CaO [50] are fragmentary and qualitative in character, and give no additional information on the behaviour of excess oxygen in MO.

3. Summary of Data on the Non-stoichiometry of BaO and SrO Specimens Having a Highly Developed Surface

The production of excess M or O in MO both in the bulk of the crystals and on their surface is the factor responsible for the sharp change in the electrophysical properties of the oxides. Thus to select conditions for the synthesis of a substance with required properties, it is necessary to know how the magnitude of the excess of a given component of the compound depends on the vapour pressure and temperature. One method of summarising this relationship is by constructing $p-T-x$ diagrams.

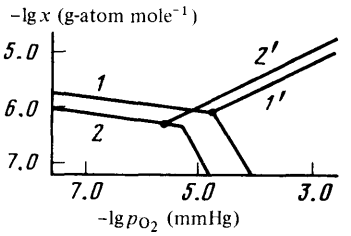


Figure 7. Dependence of the excess component in BaO on p_{O_2}:[51] *1*,*2*) concentration of excess Ba at 1150° and 1000° respectively; *1'*,*2'*) concentration of excess oxygen at 1150° and 950° respectively.

The first attempt to use the results of direct determinations of the excess of the components in BaO to construct this diagram was made by one of the present authors[51]. For this purpose, use was made of the results of measurements using powdered specimens, which are of particular interest since they are used as electron-emitting coatings in thermocathodes. Since in the production of the emitting power of these cathodes, in addition to the excess metal dissolved in the bulk of the crystals, an exceptional role is played by the excess metal localised on their surface, the coordinate reflecting the excess metal in the $p-T-x$ diagram included both the metal dissolved in the bulk of the crystals and the metal situated on the surface. This gave these diagrams the maximum utility for practical applications.

Fig. 7 shows the change in the magnitude of the excess of a component in BaO on p_{O_2} at a given temperature. Lines *1* and *2* show the magnitude of the excess Ba at 1150° and 950°, and lines *1'* and *2'* the excess oxygen at the same temperatures. Taking sections of the isotherms in Fig. 7 along the concentration axis and transferring them to coordinates $\lg p_{O_2} - 1/T$ gave the part of the $p-T-x$ diagram for the pressure range of greatest practical interest[51] (Fig. 8).

The $p-T-x$ diagram for strontium oxide (Fig. 9) was constructed similarly[45], again for specimens having a highly developed surface and for the range of small departures from stoichiometry.

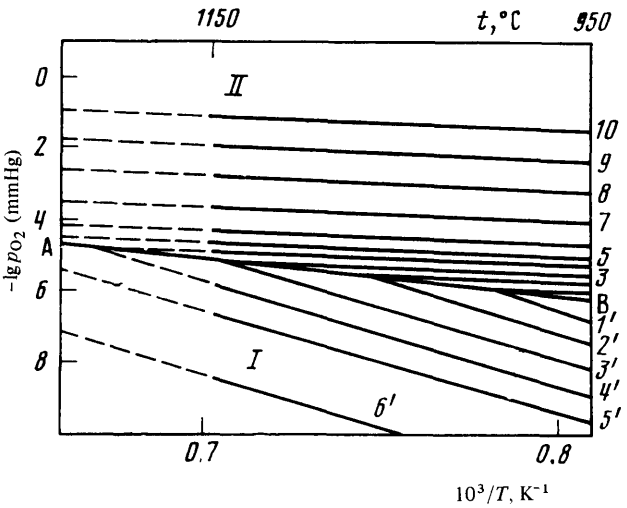


Figure 8. $p-T-x$ diagram for BaO [51] (region *I*—range of excess Ba, region *II*—range of excess oxygen). Concentration of excess components: *1*) 1.8×10^{-6}; *2*) 1.6×10^{-6}; *3*) 1.3×10^{-6}; *4*) 1.0×10^{-6}; *5*) 9.1×10^{-7}; *6*) 7.9×10^{-7}; *7*) 6.3×10^{-7}; *8*) 5.2×10^{-7}; *9*) 2.5×10^{-7}; *10*) 4.0×10^{-6}; *11*) 1.0×10^{-5}.

1. Analysis of Crystal–Vapour Equilibrium

It is of interest to determine the conditions of the crystal–vapour phase equilibrium under which: 1) the overall compositions of the vapour phase and the crystal are the same, and 2) the crystal has the stoichiometric composition.

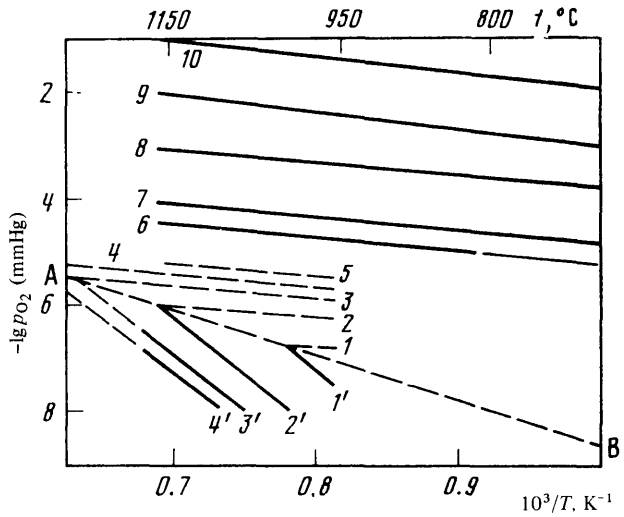


Figure 9. $p-T-x$ diagram for SrO [45] (excess oxygen above line AB, excess strontium below it). Concentration of excess components: *1*) 3×10^{-7}; *2*) 5×10^{-7}; *3*) 6.5×10^{-7}; *4*) 8×10^{-7}; *5*) 1×10^{-6}; *6*) 2×10^{-6}; *7*) 3×10^{-6}; *8*) 7×10^{-6}; *9*) 1.8×10^{-5}; *10*) 4.5×10^{-5}.

III. SOME THERMODYNAMIC PROPERTIES OF MO CRYSTALS

To investigate the nature of the non-stoichiometry of MO crystals, it is useful to draw on experience gained in the thermodynamics of solutions. Thermodynamics makes it possible to regard non-stoichiometric crystals as solid solutions in which the solvent is the main material MO, and the solutes are the excess components, the products of the dissociation of the main substance.

In the thermodynamic analysis of the properties of a non-stoichiometric phase, it is necessary to bear in mind that published data on the departures from stoichiometry do not always contain the required information on the surface area of the specimens studied. This makes it difficult to use these data, since in specimens having a highly developed surface, the magnitude of the departure from stoichiometry is determined not only by pressure and temperature but also by the degree of dispersion of the specimen. Thus the present authors selected from the available experimental data those characterising the excess of the components only in the bulk of the MO crystals, and used the methods of the thermodynamics of solutions in an attempt to analyse various thermodynamic properties of non-stoichiometric crystals and summarise the information in the form of $p-T-x$ diagrams.

With isothermal equilibrium change in the composition of an MO crystal, the vapour pressure above the specimen passes through an extremal value. At the extremal point, the overall compositions of the equilibrium vapour and solid phases are the same, so that volatilisation of the MO crystals at a given temperature can take place without change in the composition of the specimen. The relationship between the concentration of the excess components in MO crystals and the composition of the vapour at the extremal point can be examined.

MO is partly dissociated in the vapour phase. The volatilisation and dissociation of the oxide can be described as follows:

$$\mathrm{MO(solid)} \rightarrow \mathrm{MO(vapour)}, \quad K_{10} = p_{MO}/x_{MO}; \tag{10}$$

$$2\mathrm{MO(vapour)} \rightarrow 2\mathrm{M(vapour)} + \mathrm{O_2}; \quad K_{11} = (p_M^2 p_{O_2})/p_{MO}^2, \tag{11}$$

where x_{MO} is the mole fraction in the solid phase, and K_{10} and K_{11} the equilibrium constants of the corresponding reactions.

The total vapour pressure over the MO crystals is given by the sum

$$p = p_{MO} + p_M + p_{O_2}. \tag{12}$$

To find the vapour pressure extremal point, p_{MO} and p_{O_2} in Eqn. (12) are replaced by p_M, K_{10}, and K_{11}, and the right-hand side of the equation is differentiated with

respect to p_M. The expression obtained is put equal to zero, and transformed to give

$$2p_{O_2}/p_M = 1 + (K_{10} + 2p_{O_2}/x_{MO})\frac{\partial x_{MO}}{\partial p_M}. \quad (13)$$

When the excess components dissolve in MO, processes take place leading to the production of defects of various kinds in the crystal. These processes can be represented in general form as follows:

$$A_{vap} \rightleftarrows (i\,C + j\,D + \ldots + r\,E)_{cryst}, \quad (14)$$

where A represents the metal or oxygen (O_2) in the vapour phase, and C, D, ... E are the new components of the crystal, formed in its interaction with the vapour A.

At the comparatively small departure from stoichiometry observed in alkaline earth metal oxides, their phases can be regarded as very dilute solutions. In this case the equilibrium constant of reaction (14) has the form

$$K = \frac{[C]^i [D]^j \ldots [E]^r}{p_A}. \quad (15)$$

Since

$$[C] = \frac{i}{j}[D] = \ldots = \frac{i}{r}[E], \quad (16)$$

Eqn. (15) can be solved for [C]:

$$[C] = K' p_A^{1/(i+j+\ldots+r)}, \quad (17)$$

where

$$K' = \left[K\left(\frac{i}{j}\right)^j \ldots \left(\frac{i}{r}\right)^r\right]^{1/(i+j+\ldots+r)}$$

Thus the distribution of the excess components between the vapour phase and MO crystals is described in general form by the equations:

$$x_M = K_M p_M^{1/m}, \quad (18)$$

$$x_O = K_O p_{O_2}^{1/n}, \quad (19)$$

where m or n are equal to the sum of the stoichiometric coefficients in the right-hand side of Eqn. (14), or, put differently, are equal to the number of particles and quasi-particles formed in the solid phase from one metal atom or oxygen molecule on going from the vapour to the solid phase. If the particles and quasi-particles formed are regarded as independent chemical components, Eqns. (14) and (15) give the following equation, which is always applicable for a solid solution of the excess components in MO†:

$$x_{MO} + m x_M + \frac{n}{2} x_O = 1. \quad (20)$$

x_{MO} in Eqn. (13) is expressed in terms of x_M and x_O, using Eqn. (20). x_M and x_O are then replaced by their values from Eqns. (18) and (19). Since x_M and x_O are much smaller than 1, this gives the approximate equation

$$2p_{O_2} = p_M - K_{10}\delta, \quad (21)$$

where $\delta = x_M - x_O$. When the homogeneity range of the compound is extremely narrow, that is $\delta = 0$, it follows that at the point of minimum vapour pressure

$$2p_{O_2} = p_M. \quad (22)$$

From published data on the dissociation constant of MO

$$K_{MO} = K_{10}^2 K_{11} = p_M^2 p_{O_2}/x_{MO}, \quad (23)$$

where $x_{MO} \simeq 1$, it is possible to calculate p_M at the vapour pressure extremal point with allowance for Eqn. (22). At the total vapour pressure minimum

$$p_M = (2K_{MO})^{1/3}. \quad (24)$$

Eqns. (18), (19), and (22) can be used to find the vapour pressure of M over MO crystals having the stoichiometric composition at $\delta = 0$, and also the concentration of quasi-excess M and O at this point. For this purpose, Eqns. (18) and (19) are equated, and in Eqn. (19) p_{O_2} is expressed in terms of p_M, using Eqn. (23). This gives:

$$p_M = \left(\frac{K_O K_{MO}^{1/n}}{K_M}\right)^{mn/(n+2m)}. \quad (25)$$

The value of p_M at $\delta = 0$ is substituted in Eqn. (18) to obtain the concentration of quasi-excess components:

$$x_M = x_O = (K_{MO} K_O^n K_M^{2m})^{1/(n+2m)}. \quad (26)$$

The total concentrations of both quasi-excess components in the stoichiometric crystal are obviously equal to $2x_M$.

It is possible to calculate p_M at the total vapour pressure minimum, and also p_M and x_M at $\delta = 0$ for BaO. The dissociation constant of BaO is known[52]:

$$\lg K_{BaO} = -\frac{352.1 \cdot 10^3}{4.57T} + 40.54 - 3.6 \lg T, \ (\text{mmHg})^3 \quad (27)$$

Eqns. (24) and (27) are used to find p_{Ba} at the total vapour pressure minimum

$$\lg p_{Ba} = \lg(2p_{O_2}) = -\frac{117.4 \cdot 10^3}{4.57T} + 13.82 - 1.20 \lg T. \quad (28)$$

To calculate p_{Ba} and x_{Ba} at $\delta = 0$, it is necessary to know not only K_{BaO} but also K_O, K_{Ba}, m, and n. The values of K_O and n are known from Eqn. (9). The solubility of excess Ba in BaO for an infinitely dilute solution is given in general form by the equation

$$x_{Ba} = C p_{Ba}^{1/m} \exp(-A/RT), \quad (29)$$

where A, C, and m are constants. From published data, the parameter $m = 3$ [9,14,22] and $A = 5$–10 kcal mole^{-1}; [29] in the present work it was assumed that $A = 7.0$ kcal mole^{-1}, and the apparently most reliable data[14] then gave

$$x_{Ba} = 8 \cdot 10^{-4} p_{Ba}^{1/3} \exp(-7 \cdot 10^3/RT). \quad (30)$$

p_{Ba} and x_{Ba} are now obtained for $\delta = 0$:

$$\lg p_{Ba} = -\frac{120.0 \cdot 10^3}{4.57T} + 14.10 - 1.35 \lg T; \quad (31)$$

$$\lg x_{Ba} = \lg x_O = -\frac{47.0 \cdot 10^3}{4.57T} + 1.61 - 0.45 \lg T. \quad (32)$$

Comparison of Eqns. (28) and (31) shows that for BaO, the composition of the crystal at the extremal vapour pressure will differ only slightly from the stoichiometric composition, particularly at temperatures above 1000°. The value of x_{Ba} is calculated assuming that $\delta = 0$ at $p_{Ba} = 2p_{O_2}$. For this purpose, the value of p_M from Eqn. (24) is substituted in Eqn. (25):

$$K_M = 2^{-1/3} K_O (K_{MO}/4)^{1/18}. \quad (33)$$

† In the general case, the coefficients of x_M and x_O are equal to

$$\left(\frac{i+j+\ldots+r}{i}\right),$$

where $i = 1$ or 2 for the dissolution of a metal atom or an oxygen molecule respectively.

Thus

$$x_{Ba} = 1.0 \cdot 10^{-3} p_{Ba}^{1/3} \exp(-10.5 \cdot 10^3/RT). \quad (34)$$

At high temperatures, Eqn. (34) gives values of x_{Ba} close to those obtained from Eqn. (30).

Similar calculations can be carried out for strontium oxide. The expression for the dissociation constant of SrO [52] is:

$$\lg K_{SrO} = -\frac{362.0 \cdot 10^3}{4.57T} + 40.40 - 3.27 \lg T \ (\text{mmHg})^3. \quad (35)$$

The extremal vapour pressure of SrO corresponds to the following value of p_{Sr}, calculated from Eqns. (24) and (35):

$$\lg p_{Sr} = \lg(2p_{O_2}) = -\frac{120.1 \cdot 10^3}{4.57T} + 13.75 - 1.09 \lg T. \quad (36)$$

To calculate p_{Sr} and x_{Sr} at $\delta = 0$, the experimental dependence of x_O on p_{O_2}, which is more complex than that for BaO, is first analysed, The parameter n in Eqn. (19) is fractional (see Table 1), apparently indicating that oxygen is distributed by two competing mechanisms[45]. Since n is close to 2, it appears natural to assume that one of the mechanisms, probably the principal mechanism, is described by a distribution law which is similar to that for BaO and has the parameter $n = 2$. Thus the relationship between the concentration of excess oxygen in SrO and the oxygen pressure is represented in the form of the sum:

$$x_O = K_1 p_{O_2}^{1/2} + K_2 p_{O_2}^{1/f}, \quad (37)$$

where the first term on the right-hand side of the equation corresponds to the principal distribution law.

Table 2. Coefficients K_1 and K_2 in Eqn. (34).

T, °C	700	800	950	1150
$10^4 K_1$	2.6	1.9	1.2	0.64
$10^5 K_2$	2.4	3.1	2.3	2.7

Eqn. (37) gives the best description of the experimental data (practically within the range of scatter) if it is assumed that $f = 4$ (for $f = 3$, 5, or 6 greater deviations from the interpolation line are obtained). The calculated coefficients K_1 and K_2 are given in Table 2. The second mechanism makes a practically constant contribution to the value of x_O at a fixed p_{O_2}, irrespective of temperature in the range 700–1150°C. This is possible if it is assumed that the additional absorption is background absorption. The temperature dependence of the solubility of oxygen in SrO for the principal mechanism is described by the equation

$$x_O = 4.0 \cdot 10^{-6} p_{O_2}^{1/2} \exp(+9.0 \cdot 10^3/RT). \quad (38)$$

When K_O and K_{SrO} are known, it is possible to find x_{Sr} from Eqn. (33):

$$x_{Sr} = 1.4 \cdot 10^{-4} p_{Sr}^{1/3} \exp(-11 \cdot 10^3/RT), \quad (39)$$

assuming that, as in the base of BaO, $m = 3$.

At the point $\delta = 0$, the concentration of quasi-excess Sr is given by

$$\lg x_{Sr} = \lg x_O = -\frac{52.2 \cdot 10^3}{4.57T} + 1.08 - 0.41 \lg T. \quad (40)$$

Fig. 10 gives the calculated solubility isotherms for the excess Sr and oxygen in SrO at 1150°, together with experimental data[45] on the solubility of oxygen in SrO and data[28] on the solubility of Sr in SrO at high metal vapour pressures. The calculated isotherms show satisfactory agreement with the experimental isotherms obtained for other vapour pressure ranges.

2. Properties of the Solid Solution of M in MO Close to the Solidus Line

At high metal vapour pressures close to the solidus line, the concentration of excess M in MO is proportional to p_M (see Fig. 1), that is the distribution of M between the vapour and solid phases is described by Henry's law: $x_M \sim p_M$. The influence of temperature on the solubility of M in MO in this range of values of p_M can be examined. For the qualitative discussion of this question, the approximation of regular solutions can be used. In this case the activity coefficient (γ_M) is given by the equation[53]:

$$\lg \gamma_M = \alpha/RT, \quad (41)$$

where α is a constant parameter which has the significance of the differential molar heat of solution. The activity of M in the solid solution is given by the expression

$$a_M = \gamma_M x_M = p_M/(p_M^0)_{\text{solid}}, \quad (42)$$

where p_M is the vapour pressure of M above the solution of M in MO, and $(p_M^0)_{\text{solid}}$ the vapour pressure of the pure solid metal.

Substituting Eqn. (41) in Eqn. (42) gives

$$\ln x_M = -\alpha/RT + \ln[p_M/(p_M^0)_{\text{solid}}]. \quad (43)$$

The value of α calculated using data on the solubility of M in MO, given in Fig. 1, and on the saturated vapour pressure of the solid alkaline earth metals[7,25,54]. For BaO, SrO, CaO, and MgO, the calculated values of the parameter α are 14.1, 18, 19, and 33 kcal mole^{-1} respectively. Analysis of Eqn. (43) shows that if the heat of sublimation of M is greater than α, the solubility of M in MO at a given vapour pressure decreases with increase in temperature. Comparison of the values of α with the heats of sublimation, equal to 42, 36, 41, and 34 kcal mole^{-1} for Ba, [7] Sr, Ca, and Mg [54] respectively, shows that the solubility should decrease with increase in temperature for BaO, SrO, and CaO. This is confirmed by available experimental data for SrO [28] (see Fig. 1). The solubility of atoms of the alkali metals in crystals of their halides shows a similar temperature dependence[55]. For a solution of Mg in MgO, the values of the heat of sublimation and α coincide. The temperature dependence of the solubility in this case is determined by the deviations of the properties of the real solution from those of a regular solution. The solubility of Mg in MgO increases with temperature (see Fig. 1), [26] in contrast to the oxides of the other alkaline earth metals.

Fig. 11 gives the solubility isotherms for Ba in BaO, calculated from Eqn. (30) at low Ba vapour pressures and from Eqn. (43) at high pressures. In Eqn. (43) the vapour pressure over solid Ba was calculated from the equation[7]:

$$\lg(p_{Ba}^0)_{\text{solid}} = 8.34 - (9.2 \cdot 10^3/T). \quad (44)$$

Fig. 11 shows that the isotherms intersect. At the points of intersection, however, the compositions of the solid solutions, which are at different temperatures, are not the same. At a higher temperature, the excess Ba in

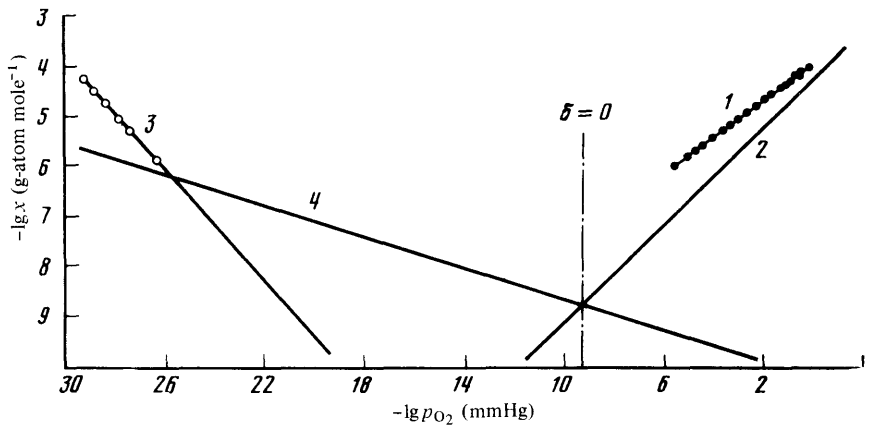


Figure 10. Solubility isotherms for excess strontium and oxygen in SrO at 1150°: *1*) oxygen solubility isotherm[45]; *2*) solubility isotherm for oxygen in the form of the complexes (O_2^{2-})(solid), calculated from Eqn. (35); *3*) Sr solubility isotherm[28], corresponding to the formation of $V_O^{\times}$; *4*) solubility isotherm for Sr in SrO, calculated from Eqn. (36) and corresponding to the formation of defects of the type $V_O^{\cdot\cdot}$ in SrO.

the solution predominates in a form corresponding to the distribution law: $x_{Ba} \sim p_{Ba}^{1/3}$. The points of intersection evidently correspond to identical total concentrations of excess Ba, which is however present in different states in BaO. A similar phenomenon should be observed for solutions of the excess metals in SrO and CaO.

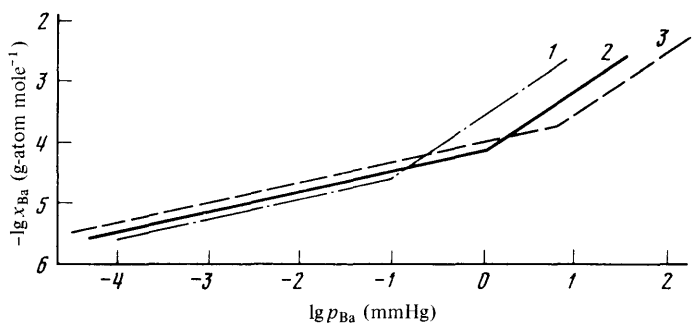


Figure 11. Solubility isotherms for Ba in BaO, calculated from Eqns. (27) and (40) for 1000° (*1*), 1200° (*2*), and 1400° (*3*).

The above discussion dealt only with the change in the properties of the solute—the excess metal—with change in the vapour pressure of M. The analysis of the behaviour of the solvent with increase in the concentration of excess metal in the solution is also of undoubted interest. The Gibbs–Duhem equation is used, with the assumption that at high vapour pressures of M, the system can be regarded as a two-component system consisting of M and MO. At a constant temperature, the Gibbs–Duhem equation has the form

$$dp = c_M d\mu_M + c_{MO} d\mu_{MO}, \qquad (45)$$

where p is the total pressure above the phases; $c_i = n_i/V$ (n is the number of moles of the component in the phase, and V the volume of the phase); and μ_i the chemical potential of the component. In the range of vapour pressure in which the solubility of M in MO obeys Henry's law, the vapour pressure of MO is smaller than p_M by many orders of magnitude[26-29,39,52]. It may therefore be assumed that $p = p_M$. Since the chemical potentials of a given component in the equilibrium phases are the same, $\mu_M = \mu_M^{vapour}$ (μ_M^{vapour} is the chemical potential of M in the vapour phase). Since the vapour phase is ideal,

$$d\mu_M^{vapour} = RT\, d\ln p_M = d\, p_M/c_M^{vapour}, \qquad (46)$$

where $c_M^{vapour} = n^{vapour}/V^{vapour}$ is the molar concentration of M in the vapour phase. Substituting Eqn. (46) in Eqn. (45) gives

$$d\mu_{MO} = \left(\frac{1-\beta}{c_{MO}}\right) p_M, \qquad (47)$$

where $\beta = c_M/c_M^{vapour}$ is a function of temperature alone, as follows from Henry's law.

Integration of Eqn. (47) gives the change in the chemical potential of the solvent with increase in p_M:

$$\Delta\mu_{MO} = \left(\frac{1-\beta}{c_{MO}}\right)\Delta p_M. \qquad (48)$$

This equation (for the change in the quantity p_{MO}) was first derived by Gibbs[56]. From the equation it follows that for $\beta < 1$, the chemical potential of MO, and hence p_{MO}, increase with increase in p_M and the concentration of excess M in MO; for $\beta = 1$, the chemical potential remains unchanged under the same conditions; and finally it decreases for $\beta > 1$. From data on the solubility of M in MO it follows that for solutions of Ba in BaO, Sr in SrO, and Ca in CaO, the parameter $\beta > 1$, so that the chemical potential of MO decreases with increase in the concentration of excess metal in the crystal. On the other hand, in the case of a solution of Mg in MgO, the parameter $\beta < 1$, and the chemical potential of MgO increases.

Thus the thermodynamic properties of a solution of excess Mg in MgO differ from the properties of solutions of the excess metal in the oxides of the other alkaline earth metals. This is quite regular, since the other physicochemical properties of magnesium oxide differ significantly from the properties of the other oxides of this homologous series[57].

3. Range of Existence of BaO on the $T-x$ Diagram

Measurements of the solubility of oxygen in BaO, carried out at low temperatures[42] (Fig. 4), give the position of the solidus line bounding the range of existence of BaO on the BaO_2 side. Fig. 12 shows that the range of existence of BaO increases with temperature, apparently as far as the eutectic temperature (~800° [58]). This part of the solidus line is described analytically by the equation[42]:

$$\lg x_O = -4333/T + 2{,}863. \qquad (49)$$

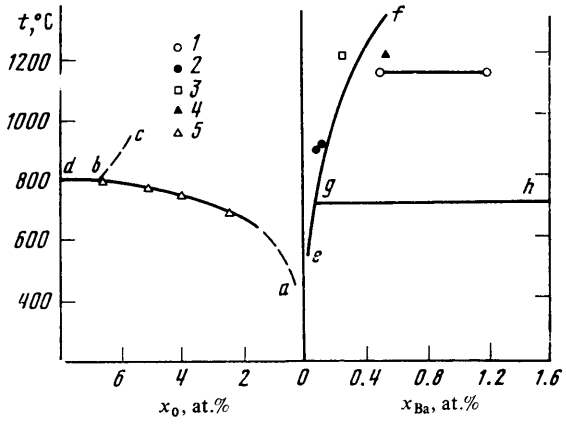


Figure 12. Range of existence of BaO (to the right of the line *abc*, to the left of the line *ef*): *1*) from Ref. 2; *2*) from Refs. 3 and 4; *3*) from Ref. 24; *4*) from Ref. 39; *5*) from Ref. 42; the lines *bd* and *gh* mark the temperatures of the eutectic reactions.

With increase in temperature above the eutectic temperature, a decrease in solubility can be expected, as a consequence of the decrease in the activity of BaO_2 in the melt in equilibrium with the phase BaO.

Several points of the solidus line bounding the range of existence of the phase BaO on the Ba side were obtained by Schriel[2], Kane[3], Libowitz[4], and others[24,35,39,40]. These data are given in Fig. 12. The temperature of the eutectic in the BaO–Ba system is ~710°.[2] Fig. 12 shows that the solubility of Ba in BaO is retrograde. To verify the degree of self-consistency of the published data[2-4,24,25,39,40], the position of the solidus line can be calculated using Eqn. (43), in which α = 14.1 kcal mole^{-1}, and $(p^0_{Ba})_{solid}$ is given by Eqn. (44). The vapour pressure of Ba over BaO crystals in equilibrium with molten Ba [2] should be much lower than the saturated vapour pressure of pure liquid Ba, since BaO is appreciably soluble in liquid Ba. To calculate p_{Ba} it is assumed that the solution of BaO in Ba is ideal. The solubility of BaO in liquid Ba is known[2]. The results of the calculation are given in Table 3. For 1200°, the calculated value of the vapour pressure of Ba, equal to 31 mmHg, is close to the measured value[39,40] (35 mmHg). The solidus calculated from Eqn. (43) is fairly close to the experimental points (Table 3 and Fig. 12).

Table 3. Solubility of Ba in BaO in contact with molten Ba.

T, °C	$(p^0_{Ba})_{liq.}$, mmHg (Ref.25)	Concn. of BaO in molten Ba, mole % (Ref.2)	p_{Ba} from liquidus line, mmHg	$(p^0_{Ba})_{solid}$, mmHg (Ref.24)	Solubility of Ba in BaO, at.%		
					calc.	exp.	refs.
900	2.4	30	1.7	2.8	0.17	0.07—0.12	3, 4
1150	38.1	42	22.0	51.3	0.34	0.5—1.2	2
1200	59.0	48	31.0	81.3	0.39	0.24	40
						0.53	39

Unfortunately, for the oxides of the other alkaline earth metals the data on the homogeneity range are even more fragmentary than for BaO. Comparison of the solubility isotherms for M in MO, given in Fig. 1, merely indicate a tendency for the solubility of M in MO to decrease in the order BaO, SrO, CaO, MgO. The same is true of the solubility of oxygen in MO, as can be seen by comparing its solubility in BaO and SrO (see Part I). Thus the range of existence of MO on the $T-x$ diagram becomes narrower from BaO to MgO.

4. $p-T-x$ Diagram of BaO

The experimental and calculated data on the solubility of the excess components in BaO can be conveniently summarised in the form of the $p-T-x$ diagram, constructed on coordinates $\lg p_{Ba} - 1/T$. This diagram is given in Fig. 13. On these coordinates, the solidus line on the Ba side at low temperatures, when the solubility of BaO in Ba is low, practically coincides with the line giving the temperature dependence of the saturated vapour pressure of pure Ba. In Fig. 13 this is taken from published data[24,25]. At higher temperatures, when the solubility of BaO in molten Ba becomes appreciable, the vapour pressure of Ba, corresponding to the solidus line, becomes lower than the vapour pressure over pure Ba. In this range, the solidus line was constructed from the calculated data given in Table 3. Part of the solidus line (the line *aa*), defining the vapour pressure of Ba in the range of equilibrium of the phases BaO and BaO_2, was constructed using Eqn. (5), which gives the value of p_{O_2} in this range. The value of p_{Ba} was calculated from the known value of p_{O_2} and the dissociation constant of BaO [52] using the equation

$$p_{Ba} = (K_{BaO}/p_{O_2})^{1/2}. \qquad (50)$$

The isoconcentrates on coordinates $\lg p_{Ba} - 1/T$ (Fig. 13) were constructed using Eqns. (4), (9), (30), and (43), describing the solubility of the excess components in BaO in different regions of the diagram. The line *bb* in the diagram is described by Eqn. (28) and corresponds to the

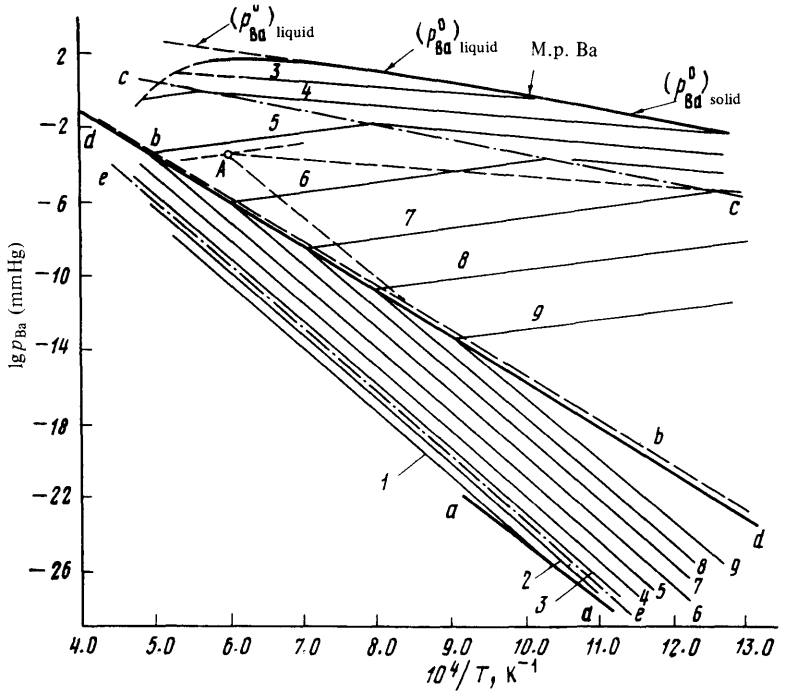


Figure 13. $p-T-x$ diagram for BaO containing excess Ba and oxygen in the bulk of the crystals. The figures at the isoconcentrates give the powers of 10^{-n}, equal to the concentration of the dissolved component.

minimum vapour pressure over BaO crystals. The line *dd* is described by Eqn. (31) and defines the conditions of existence of BaO crystals of stoichiometric composition. The line *cc* gives the change in the distribution law for excess Ba: below this line, $x_{Ba} \sim p_{Ba}^{1/3}$, and above it, $x_{Ba} \sim p_{Ba}$. Its position was calculated from the points of intersection of the isoconcentrates defined by Eqns. (29) and (43).

The isoconcentrates of the excess oxygen are given below the line *dd*. At a concentration of oxygen in BaO greater than $\sim 5 \times 10^{-3}$, the nature of the distribution of oxygen between BaO and the vapour phase changes: the solubility is described by Eqn. (4) at higher concentrations, and by Eqn. (9) at lower concentrations. On coordinates $\lg p_{Ba} - 1/T$, the isoconcentrates described by these equations are parallel to one another. Thus the change in the distribution law takes place fairly smoothly in the concentration range 1×10^{-3}–1×10^{-2}, approximately along the line *ee*.

The isoconcentrates given on the $p-T-x$ diagram (Fig. 13) can obviously be extended beyond the limits of the lines corresponding to the change in the predominant distribution law: *dd*, *cc*, and *ee*. For example, the BaO crystal under the conditions corresponding to point *A* in the diagram contains 8×10^{-6} excess Ba in a form which corresponds to the distribution law (29); 1×10^{-7} excess Ba in a form corresponding to the distribution law (43); 1×10^{-9} excess oxygen in a form corresponding to the distribution law (9), and finally $\sim 10^{-15}$ excess oxygen in a form corresponding to the distribution law (4).

The $p-T-x$ diagram in Fig. 13 can be used to find the conditions for preparing BaO crystals having a given concentration of excess components in a given form. The $p-T-x$ diagram illustrates the mutally unambiguous correspondence between the compositions of the non-stoichiometric crystals under equilibrium conditions and under the conditions of their preparation, completely determined by the vapour pressure of Ba (or O_2) and temperature. In particular, the diagram shows that the fact that the concentrations of an excess component, determined in crystals by chemical methods, are equal cannot be taken as a criterion indicating that the properties of the crystals are identical, since an excess of equal magnitude can be created by an excess component present in different states. The diagram also shows that the form of existence of excess components may change when the crystals are cooled from the temperature of synthesis, when breakdown of the solid solution has not yet taken place.

The $p-T-x$ diagram given in Fig. 13 is to a considerable extent a calculated diagram, and must therefore be regarded as semi-quantitative. To refine it, it is necessary to carry out additional experiments on the direct determination of the concentration of excess components and to study the coefficients of self-diffusion and electrical properties of the crystals under conditions of equilibrium with the vapour phase. A study of the diffusion of barium in BaO at temperatures greater than 1400° indicated that a change in the distribution law for oxygen between the vapour and BaO crystals is possible. The

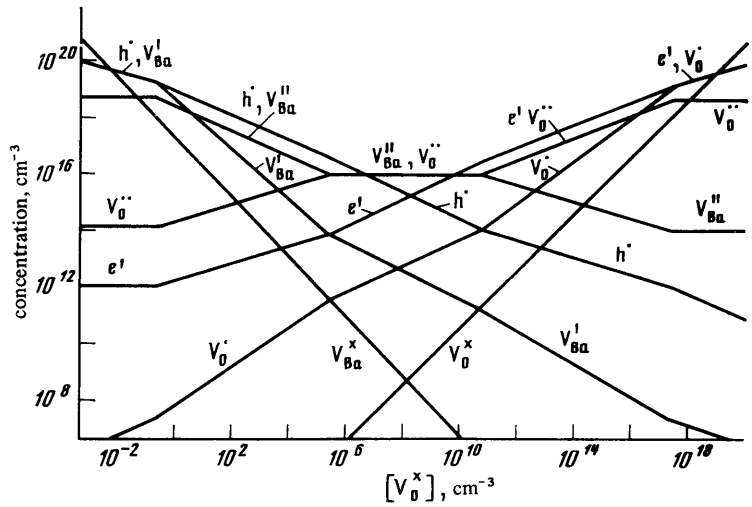


Figure 14. Dependence of the concentration of point defects in BaO on p_{Ba} at 1200° [60] for the case where $K''_S > K_i > K'_S$, where K''_S is the equilibrium constant for the formation of a pair of doubly ionised Ba and O vacancies, K'_S the same for a pair of singly ionised vacancies, and K_i the equilibrium constant for the formation of an "electron–hole" pair.

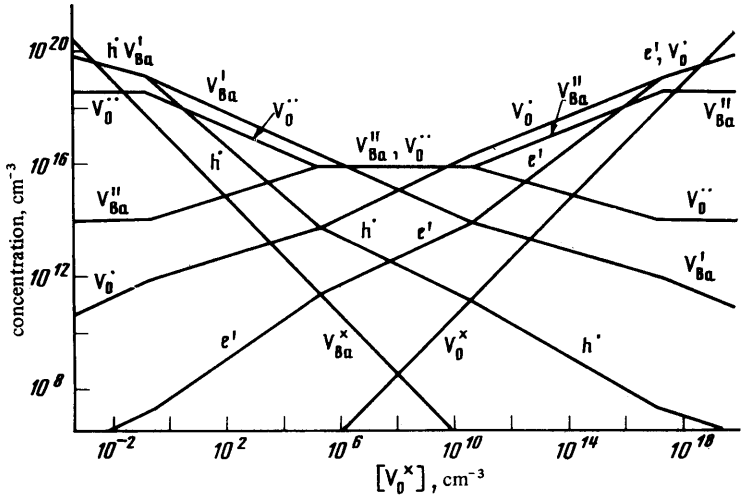


Figure 15. Dependence of the concentration of point defects in BaO on p_{Ba} at 1200° [60] for the case where $K''_S > K'_S > K_i$ (for symbols see caption to Fig. 14).

diffusion coefficient of barium under these conditions became proportional to $p_{O_2}^{1/6}$. The possibility of a change in the nature of the distribution of Ba and O_2 at low temperatures cannot be excluded.

IV. NATURE OF THE INTRINSIC ATOM DEFECTS IN MO

The electrophysical and optical properties of MO, including recent published data, have been reviewed by Kroeger[60], Kofstad[61], and Tret'yakov[62]. Kroeger gave (in the form of diagrams) two possible versions of the equilibrium for the defects in BaO; no refinements were introduced in the later reviews[61,62]. These diagrams are given in Figs. 14 and 15.

Recent papers on the direct quantitative determination of the solubility of M and O in MO give new material from which definite suggestions can be made regarding the nature of the intrinsic atomic defects in MO, and the picture of the equilibrium for defects given by Kroeger[60] can be refined.

1. Defects in BaO

The solubility isotherms for Ba in BaO (Fig. 1) show that Ba atoms dissolved in BaO at low Ba vapour pressures (below 1 mmHg at 1200°) dissociate into several particles. Under these conditions, according to published data[4,5], colour centres having a low rate of diffusion are formed, indicating that the defects produced are vacancies. This is confirmed by data[63] on the concentration of the BaO lattice and the observed[21] absence of any relationship between the absorption spectra of BaO crystals and the nature of the alkaline earth metal dissolved in them. According to Timmer[6] and Kroeger[60], the solution of Ba most probably takes place by the following mechanism:

$$\mathrm{Ba(vapour)} = \mathrm{Ba}_{\mathrm{Ba}}^{\times} + \mathrm{V}_{\mathrm{O}}^{\cdot\cdot} + 2\mathrm{e}'. \qquad (51)$$

If the condition for electrical neutrality of the crystal has the form

$$2[\mathrm{V}_{\mathrm{O}}^{\cdot\cdot}] = [\mathrm{e}'], \qquad (52)$$

then

$$[\mathrm{V}_{\mathrm{O}}^{\cdot\cdot}] \sim p_{\mathrm{Ba}}^{1/3}, \qquad (53)$$

as observed experimentally[6,39].

At higher Ba vapour pressures (above 1 mmHg at 1200°), the introduction of Ba into BaO takes place without dissociation. In the opinion of some authors[9,24], the excess Ba is situated in interstices:

$$\mathrm{Ba(vapour)} = \mathrm{Ba}_i^{\times}, \quad K_{54} = [\mathrm{Ba}_i^{\times}]/p_{\mathrm{Ba}}, \qquad (54)$$

or a solution of Ba_2O "molecules" in BaO is formed:

$$\mathrm{Ba(vapour)} + \mathrm{BaO} = \mathrm{Ba_2O}, \quad K_{55} = [\mathrm{Ba_2O}]/p_{\mathrm{Ba}}. \qquad (55)$$

The distribution law has the same form in the two cases. It can readily be seen that the nature of the distribution law is preserved if it is assumed that the solution of the excess Ba leads to the production of neutral oxygen vacancies which, like the F-centres in alkali metal halide crystals[60], are colour centres in red BaO crystals:

$$\mathrm{Ba(vapour)} = \mathrm{Ba}_{\mathrm{Ba}}^{\times} + \mathrm{V}_{\mathrm{O}}^{\times}, \quad K_{56} = [\mathrm{V}_{\mathrm{O}}^{\times}]/p_{\mathrm{Ba}}. \qquad (56)$$

Additional information is required before preference can be given to either mechanism.

As in the solution of Ba, several insertion mechanisms are observed in the solution of oxygen in BaO. At comparatively low pressures of oxygen, and hence low concentrations of excess oxygen dissolved in BaO, its concentration is proportional to the square root of the oxygen pressure (see Part II). This law should also be observed when the excess oxygen forms an atomic solid solution, and also when it dissolves in BaO as the peroxide. In the first case the following quasi-chemical reactions of solution are possible in principle[47]:

$$\tfrac{1}{2}\mathrm{O_2} = \mathrm{O}_{\mathrm{O}}^{\times} + \mathrm{V}_{\mathrm{Ba}}^{\times}, \quad K_{57} = [\mathrm{V}_{\mathrm{Ba}}^{\times}]/p_{\mathrm{O_2}}^{1/2}, \qquad (57)$$

$$\tfrac{1}{2}\mathrm{O_2} = \mathrm{O}_i^{\times}, \quad K_{58} = [\mathrm{O}_i^{\times}]/p_{\mathrm{O_2}}^{1/2}. \qquad (58)$$

Since however the heat of dissociation of oxygen molecules to oxygen atoms is large, it is to be expected that the total thermal effect of reaction (57) or (58) will be endothermic, and not exothermic, as found experimentally[43,47]. It was therefore suggested[43] that in the solution of oxygen, the formation of barium peroxide takes place preferentially:

$$\tfrac{1}{2}\mathrm{O_2} + \mathrm{BaO} = \mathrm{BaO_2}, \quad K_{59} = x_{\mathrm{BaO_2}}\gamma_{\mathrm{BaO_2}}/a_{\mathrm{BaO}}p_{\mathrm{O_2}}^{1/2}, \qquad (59)$$

where a_{BaO} is the activity of BaO, equal to ~1, and γ_{BaO_2} the activity coefficient of BaO_2 dissolved in BaO (since the solution of BaO_2 in BaO is dilute, γ_{BaO_2} is constant at a given temperature). The same conclusion was reached in later work[47].

Because of the fundamental importance of this question, the enthalpies of various processes taking place when oxygen is dissolved in BaO with the formation of a solid solution of BaO_2 in BaO will be calculated. Differentiation of the expression for $\ln K_{59}$ obtained from Eqn. (59) with respect to temperature at p_{O_2} = const gives

$$\partial \ln K_{59}/\partial T = \partial \ln \gamma_{\mathrm{BaO_2}}/\partial T + \partial \ln x_{\mathrm{BaO_2}}/\partial T. \qquad (60)$$

If both sides of Eqn. (60) are multiplied by RT^2, the term on the left-hand side of Eqn. (60) acquires the significance of the enthalpy of the reaction (ΔH_r) for BaO_2 formation, and the term $(-RT^2\partial \ln \gamma_{BaO_2}/\partial T)$ is the differential molar heat of solution of BaO_2 in BaO ($\Delta \bar{H}_{BaO_2}$). Thus from Eqn. (60) it follows that

$$\Delta H_p = -\Delta \bar{H}_{\mathrm{BaO_2}} + RT^2\partial \ln x_{\mathrm{BaO_2}}/\partial T. \qquad (61)$$

From Eqn. (9), $RT^2\partial \ln x_{BaO_2}/\partial T = -9.1$ kcal mole^{-1}, and the published[42] enthalpy of reaction (59) is −18.8 kcal mole^{-1}. Thus $\Delta \bar{H}_{BaO_2} = 9.7$ kcal mole^{-1}, and the solution of BaO_2 in BaO is endothermic, as expected from the large positive deviations from ideal behaviour shown by the solution of BaO_2 in BaO. The overall heat of solution of oxygen in BaO is exothermic, however, because of the large exothermicity of reaction (59).

According to Swalin and coworkers[47], reaction (58) indicates that combined pairs of oxygen atoms are formed in the BaO lattice

$$\tfrac{1}{2}\mathrm{O_2} + \mathrm{O}_{(\mathrm{solid})}^{2-} = (\mathrm{O_2^{2-}})_{(\mathrm{solid})} \qquad (62)$$

(O^{2-}(solid) is the anion in the site of the BaO crystal lattice), and these pairs should be arranged along the (100) direction in the BaO crystal lattice. In the opinion of the authors cited[47], the formation of these complexes should lead to expansion of the BaO crystal lattice. Their calculated expansion practically coincides with that found experimentally by X-ray diffraction. The complexes (O_2^{2-})(solid) are apparently analogous to the combined pairs of oxygen ions in the crystal lattice of BaO_2.[64] The two O^{2-} ions in the complex are identical, as a consequence of a slight displacement of the O^{2-} ion in the lattice site when the complex is formed.

The equilibrium constant of reaction (62) has the form

$$K_{62} = [(\mathrm{O_2^{2-}})_{(\mathrm{solid})}]/p_{\mathrm{O_2}}^{1/2}. \qquad (63)$$

Thus $[(O_2^{2-})(\mathrm{solid})] \sim p_{O_2}^{1/2}$, which corresponds to the experimentally observed dependence of the solubility of oxygen on p_{O_2}. Recent measurements[59] of the coefficient of self-diffusion of Ba in BaO at comparatively high pressures of oxygen confirm mechanism (62). At 900–1400°, the coefficient of self-diffusion of Ba is independent of p_{O_2} in the range of pressures studied, 1×10^{-5}–1 atm.[59]

At high concentrations of oxygen in BaO (directly adjacent to the solidus line), the distribution law for oxygen between BaO and the vapour phase changes (see Fig. 13). This is apparently due to enlargement of the complexes (O_2^{2-})(solid) and the formation of "molecules" of the type $(BaO_2)_2$ in solution:

$$\mathrm{O_2} + 2\mathrm{BaO} = (\mathrm{BaO_2})_2, \quad K_{64} = [(\mathrm{BaO_2})_2]/p_{\mathrm{O_2}}. \qquad (64)$$

The expression for K_{64} shows that in the case of reaction

(64), the concentration of excess oxygen will be proportional to p_{O_2}, in agreement with experiment[42]. It should be noted, however, that although the experimental data and thermodynamic calculations lead to the conclusion that the reaction of oxygen with MO involves mainly processes leading to the formation of electrically neutral defects in the form of the complexes (O_2^{2-})(solid) and $2(O_2^{2-})$(solid) or, which is the same thing, BaO_2 and $(BaO_2)_2$, this does not prove that reactions (57) and (58), leading to the formation of an "atomic" solution of oxygen in MO, or processes of ionised defect formation[65,66], do not take place. The experiment indicates merely that processes (62) and (64) predominate.

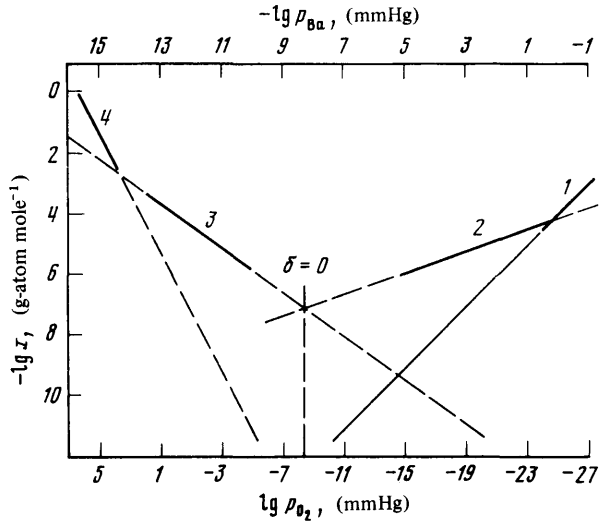


Figure 16. Solubility isotherms for excess Ba and oxygen in BaO at 1200°: *1*) $V_O^{\times}$, *2*) $V_O^{\cdot\cdot}$, *3*) complexes (O_2^{2-})(solid), *4*) complexes $(2O_2^{2-})$(solid).

Fig. 16 gives the solubility of defects of different kinds in BaO at 1200°. The equilibrium diagram for the defects in SrO, given in Fig. 10, is similar. This is quite regular, since BaO and SrO show closely analogous physicochemical properties. This is confirmed by direct measurement of the dependence of the concentration of the excess components on the vapour pressure of metal or oxygen and on temperature, and also by the study of the diffusion of Sr in SrO [67] and of Ba in BaO,[59] and by the absorption spectra of additively coloured crystals of SrO [28] and BaO.[29] These data, and the data for alkali metal halide crystals[60], indicate that the types of intrinsic point defect are similar in crystals of substances in the same homologous series.

The equilibrium diagrams for the defects in MO, given in Figs. 16 and 10, differ considerably from those proposed by Kroeger (see Figs. 14 and 15). Among others, two differences are particularly important: the first concerns the nature of the defects in an MO crystal having the stoichiometric composition, and the other is related to the fact that electrically neutral defects predominate in MO. These differences will be discussed in more detail.

2. Defects in Crystals of Compounds Having the Stoichiometric Composition

According to the hypothetical picture of the equilibrium for defects in BaO, proposed by Kroeger[60], the stoichiometry of BaO is due to the fact that the concentrations of V''_{Ba} and $V_O^{\cdot\cdot}$ or V'_{Ba} and $V_O^{\cdot}$, formed as a result of thermal disorder in the BaO crystal, are equal. The diagrams in Figs. 14 and 15 show that on coordinates $\lg x_i - \lg kp_M$ (where $kp_M = [V_O^{\times}]$), the solubility isotherms for V''_M and $V_O^{\cdot\cdot}$ (or V'_O and $V_O^{\cdot}$) exhibit mirror symmetry with respect to the straight line drawn perpendicular to the abscissa through the point of intersection of these isotherms (at which $\delta = 0$). The symmetry of the isotherms is characteristic of all the diagrams proposed by Kroeger[60] to illustrate the dependence of the concentrations of defects on the vapour pressure of the components in compounds of the type MO. This unavoidably leads to a situation in which, under conditions in which the crystal has the stoichiometric composition, the ratio of the concentrations of defects of "opposite" kinds, ensuring the symmetry indicated, should remain the same as that obtained in the examination of the so-called "internal thermal disorder" in the case where its production is not associated with interaction between the components of the crystal and the external medium[61]. In this approach (for example in the case of Frenkel disorder), the ratio of the concentrations of vacancies and interstitial atoms should be 1 : 1.

This idealised picture is far from reality. As correctly noted by Swalin[94], this relationship is not in fact necessary, and the concentration of vacancies may show absolutely no correlation with the concentration of interstitial atoms. The surface of the crystal may act as an independent source of vacancies, and the surrounding medium as a source of interstitial atoms. These considerations are also applicable to alkali metal halide crystals, which are usually regarded as model objects. In spite of the fact that in crystals having the stoichiometric composition, Schottky disorder, for example of the type[60]:

$$V_K^{\times} + V_{Cl}^{\times} \rightleftarrows O$$

is postulated, $V_{Cl}^{\times}$ and $(V_K^{\times})_2$ have been detected experimentally[60] under conditions of thermodynamic equilibrium between alkali metal halide crystals and their vapour, whereas $V_K^{\times}$ have not been found.

Similarly, it follows from the above experimental data that the stoichiometry of BaO is due to the fact that the concentrations of "unsymmetrical" defects, assumed to be $V_O^{\cdot\cdot}$ and (O_2^{2-}), [7,43,47,60] are equal. Studies of the mechanism of formation of defects in alkaline earth metal oxide crystals[11-14] have shown that their surface is the source of the defects existing in the bulk of the crystals.

Thus the existence of pairs of "symmetric" defects of the Schottky[69], Frenkel[68], or anti-structural[60] types, which are assumed to ensure the stoichiometry of the crystals, is not essential. Neither one-component nor multi-component crystals should be regarded as closed thermodynamic systems. As is usually done in the analysis of the phenomenon of departure from stoichiometry, for any crystals the formation of defects should be regarded as involving heterogeneous reactions including the exchange of material between the bulk of the crystal, its surface, and the coexisting phase (for example vapour). Under conditions of thermodynamic equilibrium,

both the composition of the bulk of the crystal and the composition of its surface layer are determined unambiguously by the temperature and composition of the equilibrium vapour phase.

3. Electrically Neutral Defects in MO

Studies of MO have shown that over a wide range of pressures and temperatures, the compositions of the compounds are determined chiefly by the concentration of electrically neutral defects, which are equivalent to atoms and molecules of the substances detected in the phases conjugate with MO. This last feature indicates that the chemical individuality of the components may be preserved on going from the conjugate phase to the dilute solution based on MO, and this makes it possible to reach certain conclusions regarding the nature of the electrically neutral defects in crystals of chemical compounds. The solid phase of a compound AB should apparently contain, albeit in extremely small quantities, all the components conjugate with it in the original system of phases[70]. When dissolved in AB, these components are electrically neutral defects, and under certain conditions, some of them may be present in appreciable concentrations (for example, Ba and BaO_2 in BaO). In the general case, the number of types of these electrically neutral defects (S) should be equal to the number of individual substances present in the phases conjugate with AB (and AB itself):

$$S=K+r,$$

where K is the number of independent components of the system, and r the number of independent chemical reactions.

Thus if the substances present in the phases in equilibrium with MO are known, it is possible to predict the types of possible electrically neutral defect in MO. Using data on the enthalpy and entropy of the reactions by which these substances are formed, it is possible in a number of cases to determine the conditions under which the appearance of significant quantities of the electrically neutral defects corresponding to these substances is possible. For example, the two possible mechanisms for the insertion of oxygen into MO: as MO_2 (see Eqn.(59)) and in atomic form (see Eqns. (57 and (58)), can be examined. As shown above (see Eqn. (61)):

$$\frac{\partial \ln x_{MO_2}}{\partial T} = (\Delta H_p + \Delta \bar{H}_{MO_2})/RT^2.$$

Similarly, for the solution of oxygen in atomic form,

$$\frac{\partial \ln x_O}{\partial T} = (\Delta H_{diss} + \Delta \bar{H}_O)/RT^2,$$

where ΔH_{diss} is the heat of dissociation of O_2 molecules to form atoms, and ΔH_O the differential molar heat of solution of atomic oxygen in MO.

As a rule, the heats of solution of the products of a chemical reaction in one another are small compared with the heat of the chemical reaction. Thus the temperature dependence of the solubility of the excess oxygen is determined by the sign of the enthalpy of the corresponding chemical reaction. When the excess oxygen dissolves in MO as MO_2, then $(\partial \ln x_{MO_2}/\partial T) < 0$, since $\Delta H_r \ll 0$. For the solution of atomic oxygen, it is to be expected that $(\partial \ln x_O/\partial T) > 0$, since $\Delta H_{diss} \gg 0$. Thus increase in temperature should lead to an increase in the concentration of atomic oxygen in the solid solution and a decrease in the concentration of MO_2. At high temperatures, the former may predominate; in this case the solubility isobar obtained on coordinates $\ln x_O - 1/T$ may pass through a minimum.

Analysis of the equilibrium constants of the reactions involved in the formation of the electrically neutral defects shows that the concentration of all types of electrically neutral defects formed by the introduction of excess oxygen increases with increase in p_{O_2}; similarly, the concentration of electrically neutral defects corresponding to excess Ba increases with increase in p_{Ba}. Close to the solidus line, the composition of the compound is determined chiefly by the concentration of electrically neutral defects. In fact, the separation of a new phase should probably be preceded by the formation of its nuclei within the original phase in the form of electrically neutral defects (one-particle or complex), corresponding to atoms and molecules of the substance being liberated.

V. PROPERTIES OF THE SURFACE AND THE NATURE OF THE EMITTING POWER OF MO CRYSTALS

Studies devoted to the investigation of the physicochemical character of the emitting power of an oxide cathode have a long history, but there is still lack of agreement on this question. One of the most fundamental problems still concerns the role of the bulk and surface properties of MO crystals in the phenomenon of the production of emitting power in the cathode. A widely encountered view, reflected in a number of monographs and reviews[71-73], is that an oxide cathode can be regarded as a semiconductor, the work function of which is determined by the concentration and energy state of the donor centres in the bulk of the crystal. A less widespread view is that the surface plays a decisive role in the phenomenon of electron emission from an oxide cathode[11,12,74-76]. The appearance of new data on the composition of the surface of MO crystals[36,37] and on the influence of the vapour of the alkaline earth metals on the emission and electrical conductivity of an oxide cathode[13,14,77-79] gives grounds for a more detailed examination of the relationship between the emission properties of a cathode and the properties of the surface of its oxide coating.

1. Non-stoichiometry of the Surface of MO Crystals

Experimental proof of the preferential localisation of excess M on the surface of MO crystals under the operating conditions of an oxide cathode were first obtained by the authors of the present review[31,32] and later by others[11,33]. A systematic study was made of the adsorption isotherms for Ba on the surface of BaO and for Sr on the surface of SrO [36,37] at 1000° and 1150° under conditions in which the pressure of oxygen over MO was greater by 4–6 orders of magnitude than the vapour pressure of M (calculated from Eqn. (50)) (the results are described above and given in Figs. 2 and 3). In spite of this, no significant adsorption of oxygen on the oxide surfaces was observed[36,37,47]. Thus in the analysis of the isotherms for the adsorption of M on MO it was possible to neglect the presence of oxygen.

Examination of various equations for the adsorption isotherms showed that the experimental data can be described by Temkin's equation for the adsorption isotherms for the case of a non-uniform surface[38]:

$$\Gamma_M = A \lg p_M + B, \quad (65)$$

where Γ_M is the quantity of adsorbed substance, g-atom cm^{-2}; and A and B are constants at a given temperature. The equations for the adsorption isotherms, given in Fig. 17 on coordinates $\Gamma_M - \lg p_M$, have the form

$$\Gamma_{Ba} = 7.7 \cdot 10^{-13} \lg p_{Ba} + 3.8 \cdot 10^{-12}; \text{ (at 1000° for Ba on BaO)}; \quad (66)$$

$$\Gamma_{Ba} = 9.4 \cdot 10^{-13} \lg p_{Ba} + 10.0 \cdot 10^{-12} \text{ (at 1150° for Ba on BaO)}; \quad (67)$$

$$\Gamma_{Sr} = 6.6 \cdot 10^{-3} \lg p_{Sr} + 8.7 \cdot 10^{-12} \text{ (at 1150° for Sr on SrO)}. \quad (68)$$

The isosteric heat of adsorption[38] of Ba on BaO, estimated approximately from two isotherms, is given by the equation:

$$q_{st} = 1.5 \cdot 10^2 (1 - 3 \cdot 10^{15} \Gamma_{Ba}) \text{ (kcal mole}^{-1}\text{)}. \quad (69)$$

Temkin's isotherm equation is applicable only if the experimental data on coordinates $\Gamma_M - \lg p_M$ are approximated by a straight line and if the slopes of the isotherms are proportional to the absolute temperature and the dependence on Γ_M is linear[38]. These requirements are met approximately by the isotherms for the adsorption of M on MO.

The adsorption of M on the surface of MO can be regarded as the solution of the excess metal in the surface layer of MO to a thickness of 1–3 molecular layers (this is the usual procedure in the analysis of the composition of the surface of solutions[80]). The concentration of M on the surface, calculated for one monolayer of MO ($x_M^{surface}$) is of the order of 10^{19} cm^{-3} (see Fig. 17). Under the same conditions, the concentration of excess M in the bulk of the crystals of BaO and SrO is only 10^{14}–10^{16} cm^{-3}.

For an understanding of the electronic processes taking place in MO specimens having a highly developed surface, it is important to compare the changes in the compositions of the surface and the bulk of MO crystals with change in the conditions of their equilibrium with the vapour of their own components. It may be assumed beforehand that the surface of the crystal contains both excess metal and oxygen in adsorbed form. This makes it possible to apply to the description of the composition of the surface the concept of departure from stoichiometry. The adsorption isotherms in Fig. 17 show that the concentrations of the excess adsorbed metal and oxygen may become of similar magnitude at values of the vapour pressure of M at which $\Gamma_M \simeq 0$. In a first approximation, it is assumed that at this point the concentrations of the quasi-excess components (M and O) on the surface are the same, that is that the surface has the stoichiometric composition. The surface is apparently enriched in excess metal at high values of p_M, and in oxygen at low values.

Comparison of Figs. 13 and 17 shows that at certain vapour pressures, not only the magnitude but also the sign of the departure from stoichiometry in the MO crystals may be different in the bulk and on the surface. The point corresponding to the stoichiometric ratio of the concentrations of quasi-excess M and O dissolved in the bulk of the crystal lies at much lower oxygen pressures than the analogous point for the quasi-excess components localised on the surface. From this it follows, in particular, that in a certain range of values of p_{O_2}, the conductivity of the crystal close to the surface may be different in character from that in the bulk: the surface is enriched in donors, whereas the bulk may be enriched in acceptors.

This phenomenon, described as inversion of the conductivity[81], has been observed experimentally for a number of semiconductors. Measurements of the electrical conductivity (σ) of polycrystalline specimens of alkaline earth metal oxides[82,83] and their solid solutions[84] showed that the isotherms giving the dependence of σ on p_{O_2} (Fig. 18) have a minimum, which corresponds to the point at which the conductivity of the oxide changes sign (if it is assumed that the mobilities of the holes and electrons are the same). Since the concentration of donor centres in the bulk of the MO crystals under the conditions of the measurements was extremely low, the high value of the

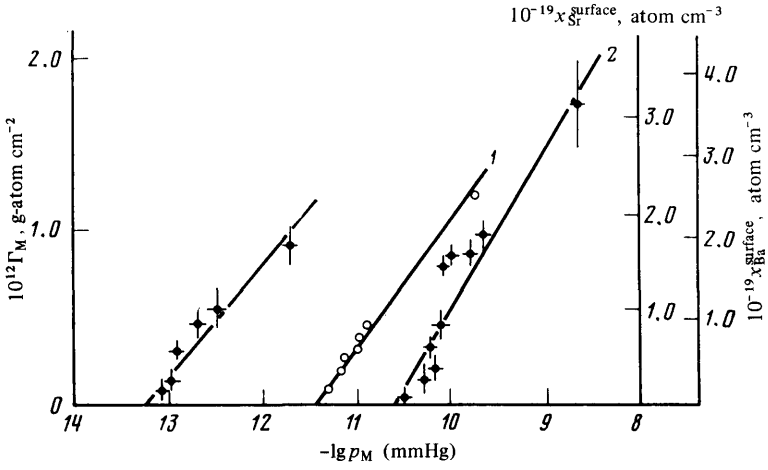


Figure 17. Isotherms for the adsorption of M on MO: *1*) Ba on BaO at 1000°;[36] *2*) Ba on BaO at 1150°;[36] *3*) Sr on SrO at 1150°.[37]

n-type conductivity could only be due to surface donor centres. Thus the minimum point on the graph giving the dependence of σ on p_{O_2} should have been situated in the range of oxygen pressures corresponding to a sharp decrease in the adsorption of M. Comparison of the experimental dependence of the electrical conductivity of BaO on p_{O_2} [82] (Fig. 18) with the p–T–x diagram of BaO for specimens having a highly developed surface (Fig. 8) supports this suggestion. The comparatively small difference (1.5–2 orders of magnitude) between the values of p_{O_2} corresponding to the stoichiometric point on the diagram in Fig. 8 and the electrical conductivity minimum in Fig. 18 may be associated with differences in the degree of ionisation of the donors and acceptors, and a difference in the mobilities of the electrons and holes.

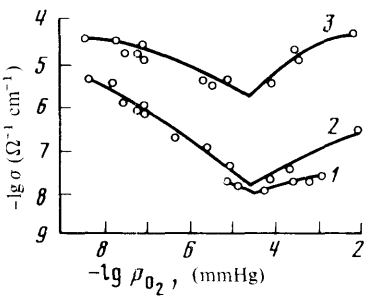


Figure 18. Dependence of the conductivity of BaO on p_{O_2}:[82] *1*) at 617°, *2*) at 637°, *3*) at 757°.

2. Nature of the High Emitting Power of MO Crystals

The adsorption of M on the surface of MO crystals is characterised by a high isosteric heat of adsorption, which is strongly dependent on the degree of covering of the surface. This is characteristic of the processes of chemisorption on semiconductors[81], when the points of adsorption on the surface of the adsorbent are energetically non-equivalent. The adsorption of M on MO may be expected to lead to the formation, on the surface, of several types of donor centre, for which the positions of the energy levels relative to the energy level of electrons in a vacuum will be different[75]. According to Vol'kenshtein[81], the high concentration of donors ($\sim 10^{12}$ cm^{-2}) on the surface of MO crystals makes it possible to regard it, from the viewpoint of its electronic properties, as "quasi-insulated" from the bulk. The existence of these surfaces was first predicted theoretically by Bardeen[85], and it has also been detected experimentally for a number of semiconductors; the work function of electrons from a semiconductor is independent of the position of the Fermi level in the bulk[81].

The conclusion that the surface of MO crystals plays a decisive role in the production of the emitting power of an oxide cathode, which follows from the results of adsorption measurements, is confirmed by studies[13,14,77–79,86–90] of the influence of the vapour of the alkaline earth metal or oxygen on the emission of a cathode and on the high-temperature electrical conductivity of the oxide coating of the cathode.

Nikonov and Beinar[13,14,78] made a detailed study of the emission of oxide cathodes in Ba vapour. The influence of a stream of Ba having an intensity of 1.2×10^{11}–1.6×10^{12} atom cm^{-2} s^{-1} on the emission current of oxide cathodes at 560–1350 K was studied[13]. At low temperatures, when the rate of deposition of Ba on the surface of the oxides of different alkaline earth metals was greater than the rate of its desorption, and the degree of covering of the surface by Ba atoms was much greater than that in the absence of the stream of Ba, a very marked increase in the emission current (I_e) was observed. At high temperatures, when the ratio of the forward and back streams of Ba changed, its influence on the emission decreased sharply, and finally disappeared at the highest temperatures. Measurements[14] at low Ba streams showed that I_e is directly proportional to the concentration of Ba atoms on the surface of the oxide coating (Fig. 19). Similar results were obtained when I_e for oxide cathodes was measured in a stream of Ba.[86–90]

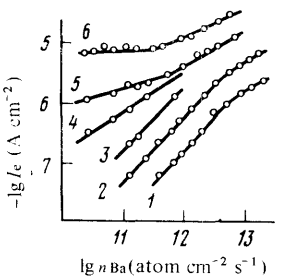


Figure 19. Dependence of the thermo-electronic emission current (I_e) of SrO on the magnitude of the stream of Ba vapour at different cathode temperatures: *1*) 317°, *2*) 347°, *3*) 422°, *4*) 482°, *5*) 537°, *6*) 607°.[13]

In contrast to the above measurements of emission, carried out under obviously non-equilibrium conditions, the influence of Ba on the properties of an oxide cathode has also been studied[77–79] under conditions close to equilibrium. Studies of the dependence of the emission current of an oxide cathode on p_{Ba} [79] showed that I_e changes very little with change in p_{Ba} (Fig. 20). Similar results were obtained in a study[77] of the electrical conductivity and thermo-e.m.f. of a BaO coating. The study[77] was based on the assumption[91,92] that at high temperatures (>800 K), the electrical conductivity of the porous coating of an oxide cathode is determined by free electrons emitted by the granules in the pores of the coating; a correlation should therefore exist between the electrical conductivity of the coating and the emitting power of the cathode. Measurements showed that at temperatures higher than 700°, the electrical conductivity (and also I_e [79]) increase very little with change in p_{Ba} from 8×10^{-7} mmHg to 2×10^{-5} mmHg. Under the same conditions, the thermo-e.m.f. of the oxide coating was only 150–200 μV K^{-1}. This value is typical of semiconductors in which the Fermi level lies at the bottom of the conductivity zone; this corresponds[77] to a high concentration of electrons in the crystal ($\sim10^{19}$ cm^{-3}). Since the concentration of donor centres in the bulk of BaO is lower by several orders of

magnitude, it was suggested[77] that there is an appreciable concentration of defects at the surface of the BaO crystals. In fact, the above concentration of electrons in BaO crystals coincides with that found experimentally from adsorption measurements of the concentration of excess Ba on the surface of BaO (see Fig. 17). The isothermal dependence of the concentration of Ba atoms on p_{Ba} is weak and logarithmic (see Eqns. (66)–(68)), and this explains the weak dependence of I_e and σ on p_{Ba} under conditions close to equilibrium.

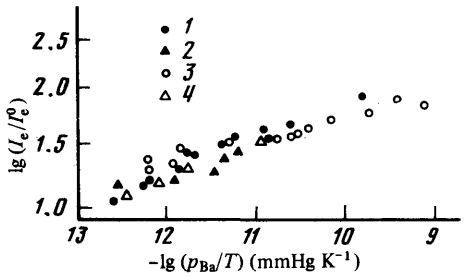


Figure 20. Dependence of the relative increase in the emission for (BaSr)O on p_{Ba} at 800° [79] from four series of experiments (*1–4*).

The change in the state of the surface of MO crystals may also provide a qualitative explanation for the phenomenon of "poisoning" of oxide cathodes by oxygen. The pressure of oxygen over BaO crystals at which a sharp decrease in the quantity of Ba atoms begins can be calculated. At 1150°, $\Gamma_{Ba} = 0$ at $p_{Ba} = 2\times10^{-9}$ mmHg, and at 1000°, $\Gamma_{Ba} = 0$ at $p_{Ba} = 2\times10^{-12}$ mmHg (see Fig. 17). The dissociation constant of BaO (Eqn. (27)) can be used to calculate the oxygen pressures corresponding to these values of p_{Ba}: at 1150°, $p_{O_2} = 7\times10^{-3}$ mmHg, and at 1000°, $p_{O_2} = 2\times10^{-5}$ mmHg. This explains the familiar experimental fact[72] that with increase in temperature, the "poisoning" of an oxide cathode takes place at higher oxygen pressures.

These experimental studies of the properties of the surface and their relationship to the emitting power of an oxide cathode apparently indicate that the state of the surface has a decisive influence on the emitting properties of alkaline earth metal oxides. In recent years, the theory of the oxide cathode having surface donor centres has been actively developed by Nikonov[75,76] and Zalm[93].

REFERENCES

1. T. P. Berdennikova, "Kolichestvennoe Opredelenie Shchelochnozemel'nogo Metalla v Oksidnom Katode. Tekhnika Zavoda "Svetlana"" (The Quantitative Determination of the Alkaline Earth Metal in an Oxide Cathode. Method from the "Svetlana" Plant), GEP, 3, 2, 6 (1932).
2. M. Schriel, Z. anorg. allgem. Chem., **231**, 313 (1937).
3. E. O. Kane, J. Appl. Phys., **22**, 1214 (1953).
4. G. Libowitz, J. Amer. Chem. Soc., **75**, 1501 (1953).
5. R. L. Sproull, R. S. Bever, and G. Libowitz, Phys. Rev., **92**, 77 (1953).
6. C. Timmer, J. Appl. Phys., **28**, 495 (1957).
7. P. V. Kovtunenko, Doctoral Thesis, D. I. Mendeleev Moscow Institute of Chemical Technology, Moscow, 1973.
8. E. B. Hensley, W. C. Ward, B. P. Johnson, and R. L. Kroes, Phys. Rev., **175**, 1227 (1968).
9. P. V. Kovtunenko and B. M. Tsarev, Radiotekhnika i Elektronika, **4**, 866 (1959).
10. B. V. Kondakov, P. V. Kovtunenko, and A. A. Bundel', Zhur. Fiz. Khim., **38**, 190 (1964) [Russ. J. Phys. Chem., No. 1 (1964)].
11. G. Ya. Pikus and V. F. Shnyukov, Fiz. Tverd. Tela, **10**, 125 (1968).
12. B. P. Nikonov and P. V. Kovtunenko, Radiotekhnika i Elektronika, **10**, 1300 (1965).
13. K. S. Beinar and B. P. Nikonov, Radiotekhnika i Elektronika, **10**, 476 (1965).
14. K. S. Beinar and B. P. Nikonov, Izv. Akad. Nauk SSSR, Ser. Fiz., **35**, 286 (1971).
15. L. R. Koller, Phys. Rev., **25**, 671 (1925).
16. E. F. Lowry, Phys. Rev., **35**, 1367 (1930).
17. A. L. Reimann and R. Murgoci, Phil. Mag., **9**, 44 (1931).
18. A. L. Reimann and L. R. G. Treloar, Phil. Mag., **12**, 1703 (1931).
19. W. Schottky, Naturwissenschaften, **23**, 115 (1935).
20. W. Heinze and S. Wagener, Z. Phys., **110**, 164 (1938).
21. W. C. Dash, Phys. Rev., **92**, 62 (1953).
22. R. T. Dolloff, J. Appl. Phys., **27**, 1418 (1956).
23. A. Smakula, Z. Phys., **59**, 603 (1930).
24. S. N. Filippov, Candidate's Thesis, Mendeleev Moscow Institute of Chemical Technology, Moscow, 1971.
25. M. P. Parshina and P. V. Kovtunenko, Zhur. Fiz. Khim., **48**, 481 (1974)[Russ. J. Phys. Chem., No. 2 (1974)].
26. L. A. Kappers, R. L. Kroes, and E. B. Hensley, Phys. Rev., **B1**, 4151 (1970).
27. W. C. Ward and E. B. Hensley, Phys. Rev., **175**, 1230 (1968).
28. B. P. Johnson and E. B. Hensley, Phys. Rev., **100**, 931 (1969).
29. J. D. Foster and E. B. Hensley, Phys. Rev., **B11**, 3966 (1975).
30. D. L. Dexter, Phys. Rev., **101**, 48 (1956).
31. B. V. Kondakov, P. V. Kovtunenko, and A. A. Bundel', Trudy Moskov. Khim.-Tekhnol. Inst., **39**, 82 (1962).
32. B. V. Kondakov, P. V. Kovtunenko, and A. A. Bundel', Zhur. Fiz. Khim., **39**, 2445 (1965) [Russ. J. Phys. Chem., No. 10 (1965)].
33. V. P. Pomazkov and P. V. Vasil'ev, Izv. Akad. Nauk SSSR, Ser. Fiz., **28**, 1354 (1964).
34. A. A. Gromov and V. A. Osipov, Zhur. Fiz. Khim., **40**, 1457 (1966) [Russ. J. Phys. Chem., No. 7 (1966)].
35. A. A. Gromov and V. A. Osipov, Zhur. Fiz. Khim., **42**, 1779 (1968) [Russ. J. Phys. Chem., No. 7 (1968)].
36. I. L. Nesterova and P. V. Kovtunenko, Zhur. Fiz. Khim., **44**, 506 (1970)[Russ. J. Phys. Chem., No. 2 (1970)].
37. I. L. Nesterova, Candidate's Thesis, Mendeleev Moscow Institute of Chemical Technology, Moscow, 1971.
38. B. M. W. Trapnell, "Chemisorption" (Translated into Russian), Inostr. Lit., Moscow, 1958.
39. P. V. Kovtunenko and M. P. Parshina, Zhur. Fiz. Khim., **48**, 36 (1974) [Russ. J. Phys. Chem., No. 1 (1974)].

40. A. A. Bundel', P. V. Kovtunenko, and S. N. Filippov, Zhur. Fiz. Khim., **43**, 1503 (1969) [Russ. J. Phys. Chem., No. 6 (1969)].
41. J. H. Hildebrand, J. Amer. Chem. Soc., **34**, 250 (1912).
42. O. V. Kedrovskii, P. V. Kovtunenko, E. V. Kiseleva, and A. A. Bundel', Zhur. Fiz. Khim., **41**, 414 (1967) [Russ. J. Phys. Chem., No. 2 (1967)].
43. T. A. Kozlenko, P. V. Kovtunenko, E. V. Kiseleva, and A. A. Bundel', Zhur. Fiz. Khim., **41**, 1118 (1967) [Russ. J. Phys. Chem., No. 5 (1967)].
44. T. A. Kozlenko, P. V. Kovtunenko, E. V. Kiseleva, and A. A. Bundel', Zhur. Fiz. Khim., **41**, 1369 (1967) [Russ. J. Phys. Chem., No. 6 (1967)].
45. P. V. Kovtunenko and T. A. Kozlenko, Izv. Akad. Nauk SSSR, Neorg. Materialy, **9**, 1514 (1973).
46. L. Till, J. Therm. Anal., **3**, 177 (1971).
47. R. B. Elo, S. P. Murarka, and R. A. Swalin, J. Phys. Chem. Sol., **34**, 97 (1973).
48. C. Holtermann. Ann. Chim., **11**, 121 (1940).
49. H. Weber, Z. Phys., **130**, 392 (1951).
50. G. D. Krotova, Candidate's Thesis, Mendeleev Moscow Institute of Chemical Technology, Moscow, 1968.
51. P. V. Kovtunenko, Izv. Akad. Nauk SSSR, Neorg. Materialy, **8**, 385 (1972).
52. A. P. Zefirov (Editor), "Termodinamicheskie Svoistva Neorganicheskikh Veshchestv" (The Thermodynamic Properties of Inorganic Substances), Atomizdat, Moscow, 1965.
53. C. D. Thurmond and J. D. Struthers, J. Phys. Chem., **5**, 831 (1953).
54. A. N. Nesmeyanov, "Davlenie Para Khimicheskikh Elementov" (The Vapour Pressures of the Chemical Elements), Izd. Akad. Nauk SSSR, Moscow, 1961.
55. H. Rögener, Ann. Phys. (Leipzig), **29**, 386 (1937).
56. J. W. Gibbs, "Thermodynamic Papers" (Translated into Russian), Gostekhteorizdat, Moscow–Leningrad, 1950, p. 212.
57. H. Remy, "Lehrbuch der anorganischen Chemie" (Translated into Russian), Vol. 1, Izd. Mir, Moscow, 1972.
58. O. V. Kedrovskii, Candidate's Thesis, Mendeleev Moscow Institute of Chemical Technology, Moscow, 1964.
59. S. P. Murarka and R. A. Swalin, J. Phys. Chem. Sol., **32**, 2015 (1971).
60. F. A. Kroeger, "The Chemistry of Imperfect Crystals" (Translated into Russian), Izd. Mir, Moscow, 1969.
61. P. Kofstad, "Non-stoichiometry, Diffusion, and Electrical Conductivity in Binary Metal Oxides" (Translated into Russian), Izd. Mir, Moscow, 1975.
62. Yu. D. Tret'yakov, "Khimiya Nestekhiometricheskikh Okislov" (The Chemistry of Non-stoichiometric Oxides), Izd. Moskov. Gos. Univ., 1974.
63. R. J. Zollweg, Phys. Rev., **100**, 671 (1955).
64. B. F. Ormont, "Struktury Neorganicheskikh Veshchestv" (The Structures of Inorganic Substances), Gostekhizdat, Moscow–Leningrad, 1954.
65. J. Rudolf, Z. Naturforsch., **13a**, 757 (1958).
66. W. D. Copeland and R. A. Smith, J. Phys. Chem. Sol., **29**, 313 (1968).
67. S. P. Murarka and R. A. Swalin, J. Phys. Chem. Sol., **32**, 1277 (1971).
68. Y. Frenkel, Z. Phys., **35**, 652 (1926).
69. W. Schottky, Z. phys. Chem., B29, 335 (1935).
70. Ya. L. Kharif and A. V. Vishnyakov, Izv. Akad. Nauk SSSR, Neorg. Materialy, **11**, 1206 (1975).
71. G. Herrmann and S. Wagener, "Die Oxydkathode" **(Translated into Russian), GTI, Moscow, 1949.**
72. **B. Ya. Moizhes, "Fizicheskie Protsessy v Oksidnom Katode" (Physical Processes in an Oxide Cathode), Izd. Nauka, Moscow, 1968.**
73. A. S. Eisenstein, Adv. Electron., **1**, 1 (1948).
74. P. Zalm, Advances in Electronics and Electron Physics, v. 25, Adad. Press, New York–London, 1968.
75. B. P. Nikonov, Izv. Akad. Nauk SSSR, Ser. Fiz., **35**, 270 (1971).
76. B. P. Nikonov, Fiz. Tverd. Tela, **15**, 1481 (1973).
77. I. N. Petrov, T. A. Dubova, G. M. Mladenov, B. Ya. Moizhes, O. V. Sorokin, and E. M. Sher, Fiz. i Tekhn. Poluprovod., **2**, 83 (1968).
78. B. P. Nikonov and K. S. Beinar, Radiotekhnika i Elektronika, **15**, 1272 (1970).
79. D. E. Anderson, Advances in Electron Tube Techniques, Pergamon Press, New York, 1961.
80. A. I. Rusanov, "Fazovye Ravnovesiya i Poverkhnostnye Yavleniya" (Phase Equilibria and Surface Phenomena), Izd. Khimiya, Leningrad, 1967.
81. F. F. Vol'kenshtein, "Fiziko-khimiya Poverkhnosti Poluprovodnikov" (The Physical Chemistry of Semiconductor Surfaces), Izd. Nauka, Moscow, 1973.
82. A. B. Kiselev and B. P. Nikonov, Radiotekhnika i Elektronika, **11**, 1886 (1966).
83. K. Hauffe and G. Traenckler, Z. Phys., **136**, 166 (1953).
84. J. Ichikawa, T. Sato, K. Chumura, and T. Sasaki, Phys. Rev., 84, 771 (1951).
85. J. Bardeen, Phys. Rev., **71**, 717 (1947).
86. T. Imai, J. Phys. Soc. Japan, **12**, 831 (1957).
87. H. J. Lemmens and P. Zalm, Philips Techn. Rev., No. 23, 19 (1961/1962).
88. R. M. Matheson, L. S. Nergaard, and R. H. Plumlee, RSA Rev., **18**, 385 (1957).
89. V. A. Smirnov and B. P. Nikonov, Radiotekhnika i Elektronika, **9**, 308 (1964).
90. R. H. Springer and D. E. Anderson, J. Appl. Phys., **37**, 4330 (1966).
91. R. Loosjes and H. J. Vink, Philips Res. Repts., **4**, 449 (1949).
92. R. Loosjes and H. J. Vink, J. Appl. Phys., **20**, 884 (1949).
93. P. Zalm, Ann. Phys. Electron. Conf. M. T. I., Cambridge, Massachusettes, 1961, M. T. I., Reports, p. 62.
94. R. A. Swalin, "Thermodynamics of Solids" (Translated into Russian), Izd. Metallurgiya, Moscow, 1967, p. 205.

Mendeleev Moscow Institute of
Chemical Technology